POLITECNICO DI TORINO

Collegio di Ingegneria Elettronica, delle Telecomunicazioni e Fisica

Master of Science Degree
Nanotechnologies for ICTs

Master Thesis

EFFECT OF ARTIFICIAL AND NATURAL WEATHERING ON INTERIOR POLYMERIC COMPONENTS OF VEHICLES

Advisors

Prof. Carlo Ricciardi

.....

Dr. Nello Li Pira

.....

Candidate

Nasim Ardeshiri

March 2021

Abstract

In this study we are going to measured and analyze solar exposure in the interior part of three different car and the aim of this study is assessing the correlation of Natural and Artificial weathering with degradation of some polymers like PC, PMMA, PP, PS, PET which are the most used inside of these cars.

In the first part of this study, we have short summary about the effect of solar irradiation (specifically UV wavelength) on some specific polymers so we will see some definition like Irradiance, Illuminance. With some International standards and special equipment, we can have artificial solar irradiation, subsequently we are going to see the effect of NATURAL and ARTIFICIAL weathering to different polymers. For our examination I need some optical parameter like Color measurement, Gloss, Haze, and Roughness for characterizing surface morphology, Adhesion for mechanical characterization evaluation.

The main objective of the second part was extracting some experimental data of our samples which I need for optical characterization and mechanical characterization and topography. I used Spectrophotometer for measuring color changes and haze, and for measuring Gloss of samples I used Gloss meter. For measuring Roughness, I used Profilometer and confocal microscope and for analyzing the Adhesion I used standard Tape which is mentioned in ISO 2409. Finally, for assessing surface topography of samples I used Confocal Microscope.

In the result and discussion part I will compare all the data that was extracted from the samples in different situation of Natural and Artificial weathering.

KEYWORDS: Artificial Weathering; Natural weathering; PC; PMMA; PET; ABS; Irradiance; Illuminance; Colour measurement; Gloss; Haze; Optical characterization; Physical Characterization; Topography Analysis; Roughness; Areal field parameters; Confocal microscope; Spectrophotometer; Profilometer.

"*Learn how to see. Realize that everything connects to everything else*"
- Leonardo da Vinci

Table of Contents

Table of Figures

Chapter 1: Introduction and Literature Review

1.1. Introduction

Nanotechnology has been implemented widely in the automotive industry. This technology is particularly useful in nanocoating, improved fabrics and structural materials, nanofluids and lubricants, tires, as well as preliminary application in smart glass/windows and video display systems. Nanocoatings have a wide range of applications in vehicles from interior to exterior. One benefit of nanotechnology has been increased resilience to scratches and wear. Polycarbonate has been a focus for traditional glass replacement due to its high impact strength, toughness, and light weight but has had difficulty in gaining real traction due to its weak resistance to scratch, abrasion, and chemicals. Wear resistance is especially important within the engine. Thus, ceramic nanostructure coatings have been used to enhance metal parts resistance by reducing the scale of size. Recent developments in the nanotechnology field have led to innovative patents for implementation in the automotive industry [1].

Polymers are nowadays clearly a material of choice in all application sectors including in Automobile sector. It is important to quantify the results of any exposure testing program. Typically, customers are interested in the number of changes that their material will experience during the exposure. Change in some properties, like color or gloss, can be measured with specialized optical measurement instruments. Changing in the other physical properties can be measured with mechanical testing and analyzing the morphology.

Automotive manufacturers have relied on new technology for vehicular accessories which are all made-up of different polymers like Poly Carbonates (PC), Poly Methyl Methacrylate (PMMA), Acrylonitrile-Butadiene-Styrene (ABS), Acrylic, glass, resin etc. Although these components offer a remarkable range of attractive properties, but the effect of climatic conditions on the durability and performance of these materials is not fully understood. The durability, performance and rate of deterioration of these products are all significantly influenced by the material composition, as well as the climatical conditions to which they are exposed. The degradation of the mechanical and optical properties of the specimen treated at different environmental conditions are a primary concern when recommending such a polymer for interior part of vehicles. The specifications of climate condition which we are using in this study are basically derived based on the data of the climatic conditions of Florida.

Literature available in this field is very rare. The literature investigation gives instructions on various types of plastic materials used in different applications and, their characteristic, usage and limited information on changes of properties due to weathering. It also gives a brief in-sight into technical papers and various studies conducted by different authors or Institutions in the field of weathering on plastic materials.

Shamsundara, B. and V, Mannikar. in their study briefly examines the effects of the weathering on the performance and properties of well-known polymers such as PC and PMMA, PET products which are most commonly used materials in automobile sector. The use of accelerated weathering techniques for assessing the stability of these product materials is also briefly discussed [2].

1.2. Weathering Test

Changes in material properties resulting from exposure to the radiant energy present in sunlight in combination with heat and water in its various states, predominately as humidity, dew, and rain. The rate of degradation of different polymers in the different condition or even in the same condition is different [3].

Weathering Testing Guidebook by Atlas Material Testing Solutions, explains the Factors responsible for weathering which includes what is weathering, factors of weathering, secondary effects, synergy, climate, measuring factors of weathering etc., It also explains the types of weathering test such as Natural testing and Laboratory testing, procedure, evaluation etc. Which also explains the weathering cycles simulates the different weathering conditions of natural weathering and their standards. This helps to researchers to select the type of testing, cycles required for simulation etc [4].

Japanese scientists show study of six of the most commonly used polymers. These were exposed to the natural weather conditions in four Japanese locations and also subjected to artificial weathering in seven test units [5]. The degradation of PVC, PMMA, ABS in a dew-cycle tester occurs much faster than in other testers. But three other polymers (PS, POM, PE), initially degrade as fast in the dew-cycle tester as they do in other testers and it is only in the last 1000 hours that the degradation of POM and PE is accelerated. This shows that the acceleration factor of dew cycle weathering apparatus is higher for some materials than for others when compared with natural weathering or with other testers. In most cases, the xenon arc Weather-Ometer and the Fadeometer give a lower degradation rate than do any of the four carbon-arc units used in the experiments. Comparison of the microphotographs of surface deterioration of specimens weathered both outdoors and in test equipment shows that the crack pattern of specimens exposed outdoors most closely resembles the crack pattern produced in a xenon arc Weather-Ometer. When specimens weathered in a xenon arc Weather-Ometer are ranked according to their degree of degradation, the order is closer to the rankings of specimens weathered outdoors than it is the ranking of specimens weathered in most of the carbon-arc units.

Ranking by the thickness of the degraded layer shows that, as is known from practice, PMMA is the clearly superior polymer. Both natural and artificial exposures confirm its stability. PS degrades twice as fast in Naha than it does in Sapporo whereas PE has similar degradation rates in both locations. This is most likely due to the fact that Naha has more rain and humidity than Sapporo and that PE is less affected by exposure to water than is PS.

The first three weathering devices do a good job of simulating the degradation which causes color changes outdoors. There is just one exception (PVC). It is difficult to explain why PVC consistently performs more poorly than PS in artificial weathering devices when, in natural exposure, it performs much better. Strangely enough, fadeometers, which are supposed to be capable of determining color stability, perform very poorly in this application.

1.3. Natural Weathering Test

Natural weathering is outdoor exposure of materials to unconcentrated sunlight, the purpose of which is to assess the effects of environmental factors like (Temperature, Humidity, UV radiation, Solar radiation, Leaf wetness). The exact weather data for a given geographic location are very important to relate weathering rate of laboratory equipment to the actual weathering rate.

Many polymeric materials are subjected to changes in mechanical properties, appearance and surface finish due to prolonged exposure to atmospheric conditions. These include effects of UV-light, temperature, humidity, oxygen and contamination and such changes may determine the service lifetime of polymeric components. Thus, sufficient knowledge of the ageing behavior of polymers in different environments is of crucial importance [6].

It is not practical to determine the weathering characteristics of materials in all of the world's climates. Therefore, benchmark climates selected for exposure testing are based on their known severity for the weathering of materials and the anticipated market of the product to that country. The major marketing area of the material should be taken into consideration when selecting suitable climates and sites for weathering tests of that country.

- ***Temperature***

Temperature's effect on material weathering includes thermal oxidation degradations and accelerating of other weathering reactions. "Rule of Thumb" is that 10°C increase in temperature doubles Rate of chemical reaction. Also, solar radiation plus high temperature equals increased rate of degradation [7].

- ***Humidity***

Measure of the amount of water in air, that can lead to physical stress. Humidity can affect both indoors and outdoors products. Often expressed as Relative Humidity (RH), where 100% is the most water that air of a given temperature can hold. Humidity is able to Changes the rate of degradation also can Changes the mode of degradation [8].

- ***Solar Radiation***

Physics of light covers all important for weathering ranges of electromagnetic radiation including UV, visible and infrared radiation. Usually described in terms of irradiance and wavelength (λ) [7].

- ***Leaf wetness***

1.3.1. Artificial Weathering Test

Accelerated weathering exposures can provide useful information in shorter time periods, but the stressors (irradiance, heat, humidity) and their intensity levels must be chosen to avoid activation of unrealistic degradation modes and failure mechanisms not seen under real world conditions [10]. The method of evaluating degradation under these conditions must also be chosen carefully to ensure identification of the same properties that are the most likely changed by natural exposure.

Laboratory Weathering Testing Methods is with Xenon Arc lamp which can simulate full spectrum of sunlight and Fluorescent UV lamp which is the best simulation of shortwave UV and possibility of water spray.

Numerous research projects have confirmed that properly filtered xenon arc radiation with full control of temperature, humidity, and rain gives good correlation with natural exposures. [11, 12]

The test protocol for weathering for various polymers, textiles, color, painting etc. is defined by different SAE and ISO standards. Indoor and outdoor weathering, facilities, light sources, etc., along with the assessment process and specifications are also defined by these guidelines [7].

The standard process ***SAE J2412*** is commonly used for checking the materials of the interior parts. A Controlled Irradiance Xenon-Arc Apparatus is used in this accelerated exposure of automotive interior trim components. The xenon long arc simulates UV and visible solar radiation when filtered properly. Irradiance, Panel Temperature, Chamber Air Temperature & Relative Humidity is needed to be controlled. The test method requires a light dark cycle of 3.8 hours followed by 1 hour dark. This loop will be repeated until the test is complete. For dark cycle there is 95% relative humidity (RH) and 50% RH during light cycle. No water spray is required for interior testing as these sections will not be expected to be exposed to rain or dew formation [13]. In the following review you will see the effect of UV and humidity on polycarbonate.

The effect of weathering and, in particular, of UV on unstabilized polycarbonate is well known. Typical signs of deterioration of polycarbonate include discoloration, embrittlement and loss of polymer strength. By exposure of different commercial PC by different molecular weights and stabilization to either natural or accelerated conditions, a maximum lifetime of three years was predicted. [14, 15, 16]

Polycarbonate was exposed in a QUV weathering panel chamber with UVA-340 nm fluorescent lamps. The moisture can affect the rate of photodegradation of polycarbonate. This study showed, at 0% RH the degradation detected was more severe. The exact mechanism by which moisture interferes with photodegradation is not known. However, the oxidized layer formed was thicker at 0% compared to 42% RH. The thicker layer of degraded polymer formed at 0% RH interferes more with the path of light than the thinner layer formed at 42% RH, resulting in lower levels of light transmission and increased levels of haze. The absence of humidity promotes the formation of a deeper layer at ambient temperature, humidity alone has no detrimental effect on PC. However, in conjunction with UV, it can affect some changes on the surface [17].

The study of ABS, PMMA and laminated safety glass under one year accelerated weathering simulation shows that their mechanical properties maintained with little changes. The laminated glass results shows that light transmission remains unchanged, and decrees of the light transmission is not really significant which contribute the performance of glass. But it is expected that on further exposure to weathering, these properties will undergo considerable changes. All materials have shown the surface effects of ageing eventually, but further exposure is required to argue whether all the materials will meet fitness for vehicle component with respect to safety during crash / impacts, aesthetics and durability [18].

Correlation of accelerated ageing data with that of outdoor exposure was carried out based on the comparison of total UV radiation energy (TUVR) needed for degradation of the Polypropylene (PP). Accelerated ageing was realized in a Q-Sun Xe-1 exposure chamber using a filtered xenon light source and a dry cycle. Weathering was carried out at Brno exposure site, representing the typical mid- European climate. It was found that if TUVR of both types of ageing is to be directly compared, accelerated ageing should be carried out at temperatures of 32–36 °C. Under such conditions, the same amount of TUVR energy induces the same extent of polymer deterioration in both types of ageing and may, therefore, be used for a reliable service life-time prediction. Data attained by means of accelerated ageing show that the more temperature is increased, the less TUVR energy is needed for the polymer deterioration [19].

The PMMA specimens were subjected to accelerated aging in a closed-loop controlled environmental chamber. The specimens are examined here at 12 and 18 cumulative months of aging. The result showed that the surface roughness has increased moreover the data in this study of formulated PMMA is consistent with the degradation mechanism of chain scission, in addition to influencing optical characteristics, the mechanism of chain scission can affect mechanical characteristic [20].

In a recent study the depletion of the UV stabilization in ethylene vinyl acetate (EVA) was observed in indoor accelerated stress testing where high UV flux was present, however, the failure mode was never observed in outdoor deployed specimens. In that study, it was concluded that the UV flux of 60 W/m^2 for 300 <λ< 400 nm was appropriate for indoor aging, whereas greater flux (e.g., 180 W/m^2) erroneously degraded the UVA within the EVA [21]. Given the limitations of indoor weathering, correlation to field degradation of materials is necessary for lifetime estimation with enhanced reliability.

Assessment of Adhesion

A strong research momentum to understand polymer adhesion in the last decade has been motivated by the growing needs of the automotive and aerospace industries for better adhesion of components and surface coatings. Adhesion is the interatomic and intermolecular interaction at the interface of two surfaces [22]. A common example of an adhesive system found in the automotive industry is the attachment of a paint coating to a polymer bumper bar. Such bumper bars are frequently made with polypropylene (PP); a material exhibiting poor surface adhesive properties in its native state [23].

Adhesion is impacted by many phenomena. The diversity and interdisciplinary nature of these phenomena made it difficult to produce a single theory or mechanism that explains the chemical and physical manifestations of the adhesion.

For assessing the adhesion of coating film of the polymer substrate I followed the American National Standards Institute (ANSI). In this method for cutting the sample, we can use Sharp razor blade, scalpel, knife or other cutting device having a cutting-edge angle between 15 and 30° that will make lattice pattern with either six or eleven cuts in each direction is made in the film to the substrate with straight hard metal, then pressure-sensitive tape is applied over the lattice and then removed, and adhesion is evaluated by comparison with descriptions and illustrations. When the coating of polymers degrades from UV exposure, its ability to protect against corrosion is reduced.

1.4. Optical Characterization of Polymers

During this experimental study I focus on interior part of three different cars, “segment A”, “segment B”, “segment D”. specifically analyzing the solar exposition and optical characterization of internal component. The different surfaces inside the cars are dashboard, DAB, cluster, radio, Gear shift, tunnel, left and right seats and the doors. First objective was comparing the spectral irradiance of sunlight inside the car with filter spectrum which is commonly used for testing aging of internal components and the second objective was the assessment of the relative illuminance between some internal components considering the different orientation and the different position inside the car.

In the first step, the amount of spectral irradiance inside the car with close windows at three different times was measured. The term "Irradiance" means a measure of radiometric flux per unit area, or flux density, Irradiance is typically expressed in W/m^2(watts per square meter).

Spectral Irradiance

Spectral irradiance is the irradiance of a surface per unit frequency or wavelength. Spectral irradiance of a wavelength spectrum is measured in W/m3 or more commonly in W/m2 nm.

Illuminance

"Illuminance" is a measure of photometric flux per unit area, or visible flux density. Illuminance is typically expressed in lux (lumens per square meter). In the following for optical characterization of our samples, mostly PC and PMMA but with different suppliers, it means different coating I was going to compare the effect of Natural Weathering and Artificial Weathering on optical properties of samples, like "Color", "Gloss" and "Haze". Polymer optical properties closely linked to our observation of a plastic product's quality and visual performance. Testing will bring you perception to fast-track development and to optimize the life cycle.

1.4.1. Color

One of the most important quality parameters in the plastics processing industry is the color [24]. Particularly in the automotive industry it is difficult to combine different dyed materials such as leather, plastic and wood. Color is an interpretation by the human brain obtained from the eye´s perception of visible electromagnetic waves [25].

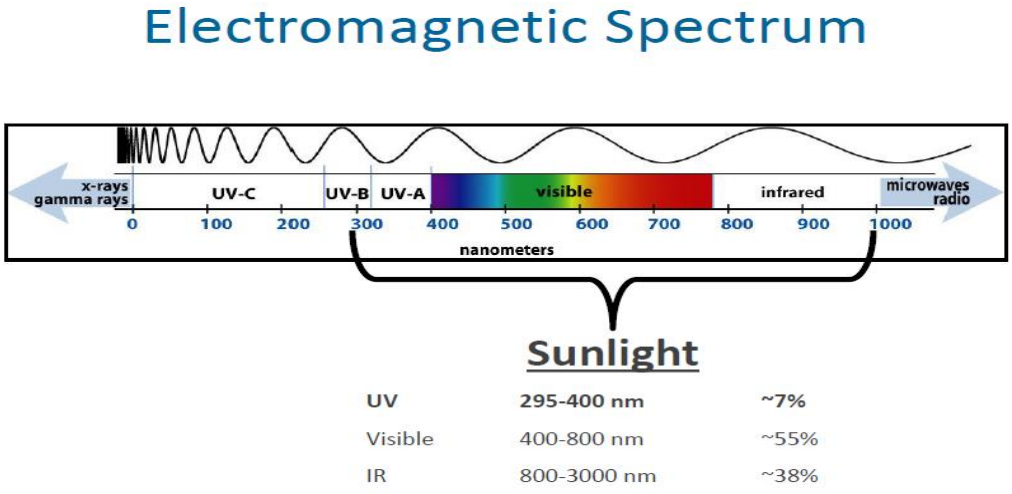

Figure 1.1. Electromagnetic Spectrum

Color measurement is based on the systems published by the Commission International de L'Eclairage (CIE). These systems derive from an understanding of the way in which the human eye and brain can process the color information. The CIE Lab represent, in a numerical form, the relevant physical values are determined: lightness (L*), red–greenness (a*) and yellow–blueness (b*) [26]. Many applications of color measurement in the examination of objects require color difference to be quantified and the shift of the color perception of an object depending on the light source, is influenced by the combination of colorant and illumination.

For this reason, the CIE introduced not only the CIE L*a*b* system but also standardized illuminants. In Europe the standard daylight illuminant (D65) is normally used [27]. There are CIE standards and units for the measurement of color difference. The basic unit of color difference is denoted by the symbol ΔE, which is defined as the distance between two points plotted in CIELab color space.

$$\Delta E^* = \sqrt{(\Delta L^*)^2 + (\Delta a^*)^2 + (\Delta b^*)^2}$$

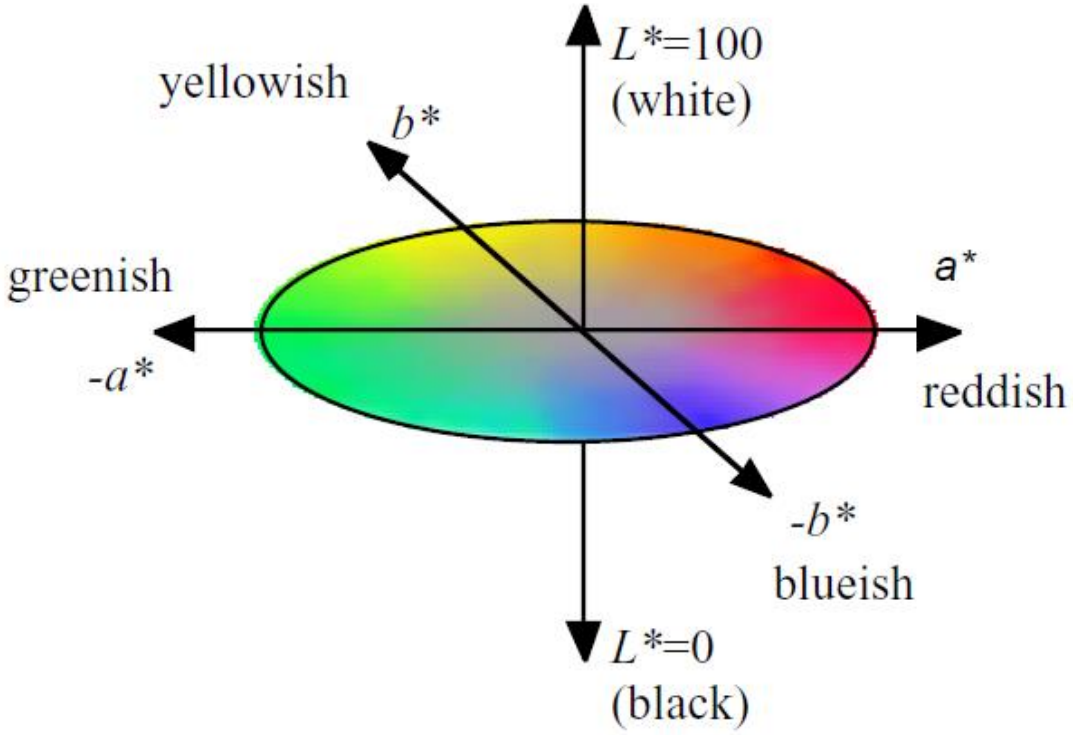

Figure 1.2. CIELab color space

1.4.2. Haze

Within the automotive industry, polymer, plastic or compound materials are tested for their perceptive properties, which describe how a product is perceived by the users regarding to their color, gloss, scratch, haze, appearance and more. I test also the Haze of our transparent samples. According to ASTM D1003-07 "Haze" give us the percentage of transmitted light which deviates from the incident light beam. Haze can be inherent in the material, a result of the molding process, or a result of surface texture. Haze can also be a result of environmental factors such as weathering or surface abrasion, resulting in poor visibility and/or glare. There are several factors responsible for light scattering such as, Surface roughness and internal optical irregularities caused by crystallization or material's level of crystallinity. Here spectrophotometers were used to measure the level of haze, light transmitting and light scattering properties of transparent materials. Haze is mostly induced by hydrolytic degradation under heat and humidity, and light only has little or no effect on its formation [28].

Note that a reduction in haze not necessarily leads to improved clarity. Haze due to surface roughness is in many cases inversely related to gloss, which is another important optical property. The haze increases uninterestingly with increasing roughness [29].

1.4.3. Gloss

Gloss is an optical property that indicates how well a surface reflects light in a specular (mirror-like) direction. It is one of the most important indicators used to describe the visual effect of an object [30]. It has been defined as 'The attribute of surfaces that causes them to have a shiny or glossy, metallic appearance.' The gloss of a surface can be greatly influenced by a number of factors, for example angle of incident light and surface topography, the smoothness achieved during polishing, the amount and type of coating applied or the quality of the substrate. [31, 32] finding the surface texture of automotive plastics is really important from the esthetical point of view, more over for safety issue a plastic surface have to be analyze, which is excessively glossy surface will reflect light and objects to a greater degree and could distract drivers while driving.

This gloss has been extensively used in the coating industry to describe the reflectance properties of a coating. The specular gloss is defined as a measure of the specular reflectance of a surface relative to the specular intensity reflected by a standard template at an angle of incidence θ:

$$G = 100\ \frac{I(\theta)}{I0(\theta)}$$

Where I is the intensity of specular reflection of the sample; I0 is the specular reflectance from the standard template; and θ could be 20◦, 60◦, or 85◦ [33].

Manufacturers design their products to have maximum application, from highly reflective car body panels to glossy magazine covers or matt finish automotive interior trim. This is especially noticeable where parts may be produced by different manufacturers or factories but will be placed adjacent to one another to create the finished product**.** Gloss can also be a measure of the quality of the surface, for instance a drop in the gloss of a coated surface may indicate problems with its cure, leading to other failures such as poor adhesion or lack of protection for the coated surface. A measurement proportional to the amount of light reflected from a surface.

The correct measurement geometry should be used according to the sample finish for matt surface 85°, mid gloss: 60° and high gloss 20°. The most appropriate angle should be selected dependent on the glossiness of the sample surface. Using the correct measurement geometry increases resolution and improves the correlation of results with human perception of quality.

Iannuzzi, G. and, Mattsson, B they presented that the gloss of the glossy surfaces of the grey specimens of ABS decreased with increasing ageing time. It is also clear that the WoM ageing had a substantially stronger effect on the surface gloss than the heat ageing (HA). In fact, the effect of the heat ageing on the gloss was quite small. This decrease in gloss would certainly have an effect on the appearance of a component, especially if it was positioned close to another component ageing at a different rate. The decrease in gloss could possibly be associated with a slight increase in surface roughness of the specimens due to weathering [34].

1.5. Morphological Characterization of Polymers

1.5.1. Roughness

Roughness is a factor of the texture of the surface. It is measured by deviations in the direction of the normal vector of the real surface from its ideal shape. If these deviations are large, the surface is rough; If they are small, the surface is smooth. However, measured (effective)

roughness is dependent on the available measurement scale and the sampling interval of the measurement technique. This makes measured roughness essentially an extrinsic property. Therefore, the relationship between roughness and measuring length scale is still an unresolved scientific problem. Roughness plays an important role in determining how a real object will interact with its environment [35].

In tribology, rough surfaces usually wear out faster and have higher friction rates than smooth surfaces. Roughness is often a good predictor of mechanical component performance, as irregularities on the surface can form cracks or corrosion sites. On the other hand, rough edges can help glue together. Roughness can be measured by manual comparison with surface coarseness (a sample of known surface roughness), but in general the surface profile is measured using a profile. They can be a contact grade (usually a diamond stylus) or optical (e.g. white light interferometer or laser scan of a confocal microscope). However, controlled roughness can often be desirable. For example, a glossy surface may be too shiny for the eyes and too slippery for the finger (the touch panel is a good example), so controlled roughness is required. This is the case when both amplitude and frequency are very important.

Specular gloss and surface roughness are important factors of coatings as they influence the visual perception of a coating on products [36]. Especially for matt coatings, these two parameters need more stringent controls [37].

Scientists and technologists expect matt films to have a very low-gloss surface as well as a micro-scale rough surface, which can impart good transparency and pleasant touch properties. As a result, many of techniques, such as an additional matting agent [38, 39] and photopolymerization [40, 41] have been widely used to construct rough surface of a coating.

Changes in polymer morphology due to UV exposure also contributed to increase the surface roughness of the samples decreasing their gloss [42]. The roughness value can be calculated on a profile (line) or on a surface (area). A wide range of roughness parameters can be used to describe a given surface [43].

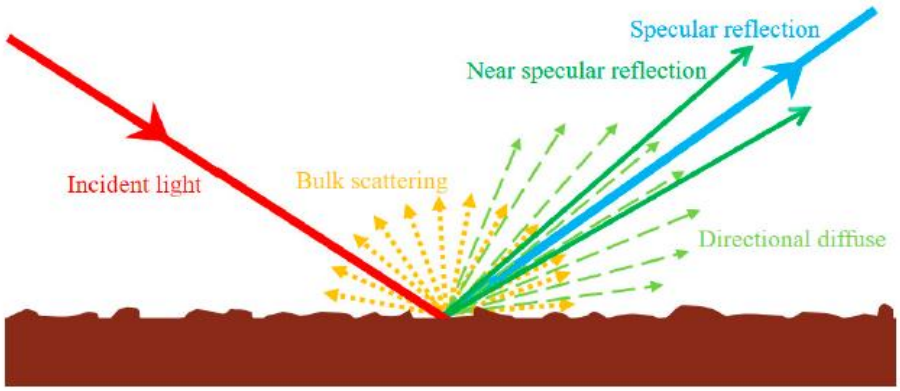

Figure 1.3. A systematic illustration of light scattering at a randomly micro rough surface.

1.5.2. Areal Field Parameter

The vast majority of surface texture parameters are the field parameters. The term field refers to the use of every data point measured in the evaluation area, as opposed to feature parameters that only take into account specific points, lines or areas. Field parameters allow the characterization of surface heights, slopes, complexity, wavelength content, etc. They are defined in the specification standard ISO 25178 [44].

The most common parameters are calculated from line profiles according to the ISO 4287 standard, but due to an increased use of 3D profilers a set of complimentary area roughness parameters have been defined in the ISO 25178 standard [45].

For better understanding of Areal Parameter, the height parameters like Ssk, Sku, Sq and Sa has been selected.

Skewness (Ssk), known as the third moment of the distribution, is used to quantify the level of asymmetry in a distribution. Skewness is negative when there is a preponderance of large data values causing the distribution to appear to have a long flat tail for smaller values. Conversely, a positive distribution is produced from data dominated by smaller values. A skewness of zero generally indicates that the distribution is symmetric about the mean [46].

$$S_{sk} = \frac{1}{S_q^3} \iint_a (Z(x,y))^3 d(x)dy$$

Kurtosis indicates the level of flatness or sharpness of the distribution. Kurtosis also known as the fourth moment of the distribution, is less than 3 when the distribution has a shorter and flatter peak compared to the ND and is greater than 3 when the distribution has a longer and sharper peak when compared to the ND. Lastly, the kurtosis is equal to 3 for the case of a normal distribution [46].

$$S_{ku} = \frac{1}{S_q^4} \iint_a (Z(x,y))^4 d(x)dy$$

Root Mean Square Height, Sq is defined as the root mean square deviation of the roughness evaluated over the calculated 3D surface [47].

$$S_q = \iint_a (Z(x,y))^2 d(x)dy$$

Arithmetic Mean Height, Sa is defined as the arithmetic mean deviation of the roughness evaluated over the calculated 3D surface [47].

$$S_a = \iint_a |Z(x,y)| d(x)dy$$

The Sa and Sq parameters are strongly correlated to each other (Blunt and Jiang2003). The Sq parameter has more statistical significance (it is the standard deviation) and often has a more physical grounding than Sa, for example, Sq is directly related to surface energy and the way light is scattered from a surface.

1.6. Polymers and Composites Commonly Used in the Automotive Industry

1.6.1. Poly (ethylene terephthalate), PET

Poly (ethylene terephthalate), PET, is a semi-crystalline thermoplastic polyester which is by far the most commonly used polyester. Its chemical formula is [C10H8O4] and the melting point is 260 °C. The glass transition temperature of PET varies between 67 ºC and 81 °C. PET polymer has commercial applications in the fabrication of various electrical instruments, packaging, X-ray sheets, plastic bottles and etc. Polyethylene has a homogenous chemical composition and divided into low- and high-density materials with a reference density of 0.94

g/cm3. Each group is highly diverse due to chain irregularities (branches), instaurations, molecular weight variations and components added during the polymerization reaction to influence basic mechanical properties and durability. PET film is a widely used material in photovoltaic module back sheets, for its dielectric breakdown strength, and in optical displays for its excellent combination of properties, notably optical clarity. However, PET degrades and loses optical clarity under environmental stressors of heat, moisture, and ultraviolet irradiance. Stabilizers are often included in PET formulation to increase its durability; however, even these are subject to degradation and further reduce optical clarity.

The band gap of irradiated PET polymer samples decreased from 3.97eV to 3.88eV with increase of time duration of UV irradiation from 0 to 40 hrs. This indicates that the conductivity of the polymer increases. Such a reduction in optical band gap may be linked to the increased conjugation due to the UV-irradiation. Further this is due to the formation of ion pairs from the bond cleavage as the energy is imparted to the covalent bonds and subsequent processes like cross linking and chain scissoring etc. In the polymers during the UV irradiation Urbach's energy values increases with the increase of irradiation time and it tells about the width of the tail of localized states within the optical band gap. The damage induced by the UV irradiations is up to small extent as evident from the shifting of the some of IR peaks of PET polymer samples [48].

Degradation of PET film under multifactor accelerated weathering exposures making haze formation by high humidity exposures. Under the heat and humidity exposures without irradiance, neither degradation mechanisms were found to be noticeable [49]. The condition in the Q-Lab QUV weathering chambers (Model QUV/Spray with Solar Eye Irradiance Control) were used for the UV light exposures (HotQUV and CyclicQUV). The QUV uses UVA-340 fluorescent lamps (280–400 nm), which closely matches the air mass (AM) 1.5 solar spectrum at the wavelengths between 280 and 360 nm. The HotQUV and CyclicQUV exposures had an irradiance of 1.55 W/m2 at 340 nm at 70˚C, comparable to approximately 3 times greater than the intensity of AM 1.5 at 340 nm [50]. The CyclicQUV exposure, per ASTM G154 Cycle 4 standard [51], is a multi-cyclic multi-stressor exposure of alternating sequences of UV light, heat, and condensing humidity designed to mimic outdoor conditions where materials are exposed to morning dew or rain followed by sunlight.

The haze formation in PET films has a number of origins, such as partial crystallinity, i.e., crystallite formation within the bulk material, which can increase due to hydrolysis induced chain scissions leading to increased polymer chain mobility and enabling rearrangement of amorphous polymer chains into ordered crystalline structures. Volumetric changes from thermal and/or mechanical expansion and contraction in the polymer matrix can cause internal stresses. These internal stresses can produce crazing and cracking in the bulk and/or on the surface, especially as more chain scissions occur due to hydrolysis and temperature cycling. These stressors can also influence the polymer morphology [52].

1.6.2. ABS

ABS or poly(acrylonitrile–butadiene–styrene) is an amorphous copolymer consisting of the thermoplastic copolymer matrix SAN (styrene–acrylonitrile) grafted onto the chains of the elastomeric phase PB (polybutadiene). ABS is widely used as an engineering polymer (vehicle interiors, domestic appliances, toys, etc.) due to its favorable mechanical properties, which combine the strength and the rigidity of the SAN phase with the toughness of the PB phase, to its good processability and to its relatively low cost. The main drawback in the usage of ABS is its limited ageing resistance, especially in outdoor applications. ABS, in fact, is subjected to

oxidative degradation which initiates when the polymer is exposed to heat (thermal oxidation), UV-light (photo-oxidation) or mechanical stress in the presence of oxygen [53, 54, 55]. Generally, it starts when sufficient energy is at hand for activating hydrogen abstraction with consequent formation of free radicals [56, 57]. Thus, the oxidative degradation of the polymer starts with the formation of free radicals ($R^{\bullet}$, $ROO^{\bullet}$, etc.) which can react with oxygen producing oxy- and peroxy-radicals, can abstract hydrogen from other polymer chains or react with each other and take part in a number of other reactions [56, 58, 59]. Some of these reactions result in chain scission and cross-linking of the rubber component which deteriorates the elastomeric properties of the PB phase leading to loss of mechanical properties, changes in chemical structure of the surface regions and surface discoloration [54, 55, 57, 60]. Some studies claim that physical ageing of the SAN phase also contributes to surface embrittlement and loss of mechanical properties [57, 58]. These kinds of reactions are normally regulated or governed by the availability of oxygen and its ability to penetrate the polymer surface, which means that the effects of the ageing are usually confined to the very surface layer of the exposed plastic component [57].

In a study by Iannuzzi, G., Mattsson, B. [61] ABS plaques were subjected to heat ageing and artificial weathering. The first consisted of heat ageing the polymer in an air-circulating oven in accordance with SS- ISO 188 at a constant temperature of 75°C. Samples of uncolored and colored ABS were taken out at different times; 500, 1000, and 1500 h. A heat ageing time of 1500 h at 75°C corresponds approximately to 5 years ageing at room temperature. This calculation was made following the Arrhenius model and assuming an activation energy of 60 kJ/mol [62, 63]. The second ageing method employed an Atlas Weather-Ometer (WoM) model 4000 which creates accelerated weather conditions. The samples were placed in a chamber in which the relative humidity was kept around 50% and xenon lamps irradiated the specimens at wavelengths between 300 and 800 nm. The light intensity was 1.2 W/m2 measured at a wavelength of 420 nm. The total color DE^* due to the ageing was significantly greater for the uncolored ABS specimens than for the gray ones. The artificial weathering produced a substantially stronger discoloration, both for the unpigmented material and the gray specimens. Later on, you will read about the changes of Gloss of ABS under this condition. The aim of this work is to investigate the impact of ageing on the surface characteristics of polymers. Such components can often be placed adjacent to other parts made of the same or other plastics. It is then important that they appear as similar as possible, and their ageing behavior must be well predicted. If the different polymers do not age at the same rate, they will look more and more different with time. This constitutes a problem for the design engineer [61].

1.6.3. PMMA

Poly(methyl methacrylate) (PMMA), also known as acrylic, acrylic glass, or plexiglass, as well as by the trade names , Plexiglas, Acrylite, , Lucite, Perclax, and Perspex, is a transparent thermoplastic often used in sheet form as a lightweight or shatter-resistant alternative to glass. It is often preferred for its moderate properties, easy handling and processing, and low cost. Non-modified PMMA is brittle when under load, especially under impact force, and is more prone to scratching than conventional inorganic glass, but modified PMMA is sometimes capable of achieving high scratch and impact resistance.

The glass transition temperature (Tg) of PMMA is 105 °C. The Tg values of commercial grades of PMMA range from 85 to 165 °C; the range is so wide because of the vast number of commercial compositions which are copolymers with co-monomers other than methyl

methacrylate. PMMA is thus an organic glass at room temperature; i.e., it is below its Tg. The forming temperature starts at the glass transition temperature and goes up from there [64].

PMMA transmits up to 92% of visible light (3 mm thickness) and reflects about 4 percent of each surface due to its refractive index (1.4905 at 589.3 nm). It filters ultraviolet (UV) light at wavelengths below 300 nm (similar to ordinary window glass). Some manufacturers add coatings or additives to PMMA in order to improve absorption in the 300–400 nm range. PMMA passes infrared light up to 2,800 nm and blocks IR with longer wavelengths up to 25.000 nm. Colored PMMA varieties allow the passage of specific IR wavelengths while blocking visible light [65].

PMMA is an economical alternative to polycarbonate (PC) when tensile strength, flexural strength, transparency, polish ability, and UV tolerance are more important than impact strength, chemical resistance, and heat resistance [66]

Mechanism of degradation may cause main chain scission in PMMA: direct main chain scission and ester side chain scission. Direct chain scission proceeds according to the following equation:

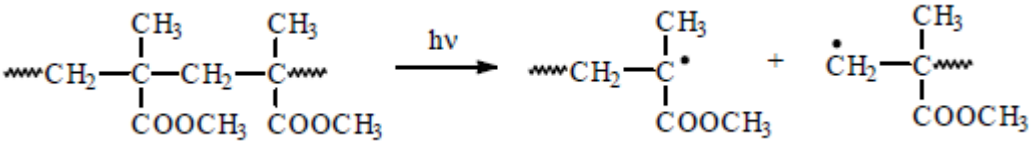

The Okazaki Large Spectrograph was used to expose PMMA samples to monochromatic radiation in the range of 250 to 1000 nm and the photoirradiated samples were studied by ESR to determine the quantum yield of the main chain scission. The direct main chain scission produces well resolved nine-line ESR spectrum. The above reaction of the direct chain scission occurs on exposure to radiation wavelength of 300 nm. Thus, this reaction can occur when PMMA is exposed to sunlight [67].

Ester side chain scission occurs in two steps. In the first step, a radical is formed by removal of the ester group. This process requires higher energy than that available in solar radiation. The reaction requires exposure to 260 and 280 nm radiation. The formation of radical is followed by a reaction in which unsaturated end-group and the radical are formed. The radicals can be oxidized and then initiate a chain of photooxidative reactions.

The presence of photoinitiators and photo accelerators changes the rates of degradation and the wavelength sensitivity. Pure PMMA must be exposed to radiation below 320 nm for degradation to occur.

Photochemical changes in PMMA are wavelength specific. In an article by Torikai and Hasegawa [68], they show that wavelength below 320 nm lowers the molecular weight of the polymer. Radiation at 260 and 280 nm is the most effective for chain scission, but relatively large changes occur on exposure to radiation of 300 nm. Above 300 nm, the rate of photolytic degradation decreases.

Exposure to water increases weight. Water has limited compatibility with PMMA but due to its small molecular size, it will penetrate PMMA by Fickean diffusion in PMMA. The study was made in conjunction with environmental stress cracking. Water was found to cause the same type of stress cracking as caused by ethylene glycol. Ethylene glycol decreases sample weight. This is because ethylene glycol extracts a minor component [69].

Miller in the study of PMMA which was reported after six months of cumulative indoor aging in the environmental chamber equipped with a xenon-arc lamp show. In detail the Specimens

were aged in a Ci4000 Weather-Ometer (ATLAS Material Testing Technology LLC), operating at the chamber temperature of 60°C and relative humidity (RH) of 60%, rendering a black-panel temperature of 100 ±7ºC. (The local conditions for transparent polymeric specimens were previously verified at 70°C and 38% RH). Specimens were placed in a carousel that rotates about a continuously operating xenon-arc lamp. Borosilicate glass filters were used to filter the lamp so that it closely replicates the AM1.5 spectrum, with the power level being controlled to 114 W·m-2 for 300≤λ≤400 nm, i.e., 2.5x the AM1.5 global spectrum [70].

Instruments such as the Ci4000 provide an ~8x acceleration factor with respect to the UV dose (where additional acceleration related to the environmental conditions of temperature and RH is location specific), based on the optical flux and duration of exposure (24 hours/day). Specimens were aged for the cumulative durations of 0, 1, 2, 4, and 6 months, where one month corresponds to 30 days. Samples of a domed Fresnel lens (spot-focus), however, were aged at 85°C and 85% RH in the dark (Blue M FRS-361F, Thermal Product Solutions Corp.), because they could not be readily fitted to the standard Ci4000 specimen trays.

Miller was observed a range in the optical and mechanical durability of the various specimens. For the most-affected specimen set, the wavelength at which the specimen became transmitting above -3dB increased from 320 to 615 nm, with an associated loss in the CPV specific photon flux density of 16% and loss in UV optical flux of 90%. In most other specimens, the cut-on wavelength remained at 390 nm, with only slight degradation of the UV transmittance. In a few specimens, the UV bandwidth was instead increased at minor expense (0.3% loss) to the CPV specific photon flux, attributed to depletion of the UV stabilization system. Particulate matter accumulated on veteran specimens decreased the CPV-specific photon flux and UV optical flux by as much as 15% and 29%, respectively. For soiled as well as optically degraded PMMA, the loss of transmittance at shorter wavelengths with time may eventually render a current- limited condition at the top cell, when multijunction technology is used.

The yellowness index of the most-affected specimen set increased linearly and loss of mass, another indicator of degradation, increased asymptotically with time. The average mass loss of 0.7% is consistent with the loss of volatile species resulting from photolytic chain scission. Separately, the contact angle was found to decrease with time, from ~70° in unaged specimens to ~50° in veteran specimens. This implies the specimens will become more easily wetted during aqueous cleaning but have become more prone to soil accumulation. The restoration of contact angle after cleaning at 6 months suggests the accumulation of water-soluble species at the surface. Such species may originate from the degradation of PMMA and/or its additives. Visual inspection identified instances of overt discoloration, crack formation, and hazing.

In the following Miller shows the specimens are examined at 12 and 18 cumulative months of aging relative to their previously reported condition at 6 months [71].

The samples were stressed in a chamber, where they were subject to the combined factors of ultraviolet (UV) light, temperature, and humidity. The study is meant to aid concentrating photovoltaic (CPV) technology, where a lens composed of PMMA is expected to achieve a 25–30-year lifetime. Various methods have been used to examine degraded PMMA specimens.

From the methods used, the dominant indoor degradation mechanism identified for the bulk of all of the formulated PMMA specimens was random chain scission. The mechanism was directly confirmed using gel permeation chromatography (where a decrease in molecular weight was observed with a negligible increase in polydispersity). The mechanism of chain scission is consistent with the results determined using: indentation (where the modulus was decreased by aging); NMR (where no new peaks were observed that would suggest cross-linking or oxidation); and TGA (where the measured activation energy suggests that the mechanism of depolymerization would occur at higher temperatures). While none of the techniques identified

a change in the chemistry of PMMA itself, NMR could be used to identify changes in copolymers and formulation additives.

The surface morphology (where erosion/roughening of the surface as well as the formation of pores and cracks were observed) and X-Ray photo electron spectroscopy (XPS) did not lend evidence towards the degradation mechanism of the bulk material. XPS did, however, suggest the formation of a hydroxyl species at the surface that may contribute to the mechanism of chain scission.

The differences between the ‘‘hazy’’ and ‘‘yellow’’ specimen categories arose from the additives used in the formulation. The profiles observed in fluorescence spectroscopy (which queries the effects of the additives as well as the degraded PMMA material) readily distinguished between the ‘‘hazy’’ and ‘‘yellow’’ specimens. The change in the optical transmittance profile for the yellow specimen (relative to a clinical grade specimen with no additives present) indicated that the UV stabilization system was depleted with age.

1.6.4. Polycarbonate, PC

Polycarbonate expressed by general formula:

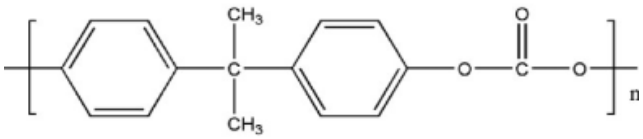

PC

It can be produced from various bifunctional alcohols, but most polymers have been manufactured using bisphenol A. polycarbonate based on bisphenol A is an aromatic compound and can, therefore, absorb UV radiation from daylight, which makes it sensitive to photolytic degradation. Exposure to UV radiation may produce many changes. The type of changes depends on radiation wavelength. The photo-Fries rearrangement is known to be a part of polycarbonate degradation.

The use of light-weight materials such as PC to produce automotive window glazings is being investigated by many OEMs in the automotive industry. Polymeric glazings are desirable because of their ability to reduce weight by up to 40%–50% and improve fuel economy while providing exceptional optics and impact resistance. The injection molding process used for PC enables breakthrough styling for innovative designs, as well as part integration which reduces cost. Clear silicone hardcoat are used to enhance the durability of the PC substrate. These coatings are used to prevent UV degradation of the PC and provide scratch resistance. Silicone hardcoats can be further enhanced to resist scratching by the deposition of a thin glass-like layer over the top of the hardcoat layer by means of Plasma Enhanced Chemical Vapor Deposition (PECVD) which provides an extremely hard, scratch resistant surface over the hardcoat [72].

Recently, Pickett studied the effect of the irradiation conditions on the weathering of engineering thermoplastics, such as polycarbonate (PC) and blends of PC with other polymers, such as ABS. The results demonstrated that the samples submitted to shorter wavelength suffer more damages. Moreover, for ABS a nonlinear correlation between irradiance and degradation was obtained [73].

Under the evaluation of polycarbonate after QUV-A radiation in the weathering panel chamber with UVA-340 nm fluorescent lamps. The emission spectra is very similar to that of sunlight for 295 <ʎ< 340 nm [74]. This radiation was considered suitable for PC, as its activation energy lies in the wavelength range of 290–350 nm, but particularly at ʎ< 310

nm. The temperature was set at 40 ±2 ○C and the RH was either 0% or 42± 5%. UV exposure was continuous for intervals up to3000 h. The result showed significant increase in haze took place in the UV-aged samples. Samples aged without UV showed less than 1% variation in haze. Whilst under UV, haze increased by about 5.5% in 2500 h of exposure.

Hence specimens exposed at 0% RH developed slightly higher levels of haze than samples aged at 42% until 1000 h, whilst after 1500 h this was reversed. with increasing periods of UV exposure, they noticed about Loss of light transmission. And**,** as samples aged without UV at various humidity levels showed no significant change in light transmission. The reduction in light transmission observed under UV was similar for the two humidity levels: approximately 5 and 4% for samples aged at 0 and 42% RH, respectively, after 2000 h of UV. As the sample turns from transparent to yellow, the polymer absorbs more visible light in the blue range, reducing the total light transmitted through the sample.

We know that also moisture can affect the rate of the photodegradation, at 0% RH the degradation detected was more severe. The exact mechanism by which moisture interferes with photodegradation is not known. However, the oxidized layer formed was thicker at 0% compared to 42% RH. The thicker layer of degraded polymer formed at 0% RH interferes more with the path of light than the thinner layer formed at 42% RH, resulting in lower levels of light transmission and increased levels of haze. [75].

For polycarbonate under the condition of mentioned in Tjandraatmadja study [75], Gloss was measured with a Gardner BYK Tri glossmeter at a 60° angle [76]. The level of surface gloss reduction being approximately 5% after 2000 h exposure. Hence the gloss reduction contributes to higher haze levels and to the reduction in direct light transmission.

1.6.5. Transparent Coating

PVD:

.

.

Lamination:

.

.

.

Transparent Composite:

In recent years, optically transparent polymer composites have been the subject of many investigations because of their novel properties and industrial applications, such as optical fiber sensors, optical isolators, packaging products, and medical devices [77, 78]. According to ASTM D 1003 standard, the transparency of, PC/SiO2, PMMA/SiO2, PS/SiO2, and PS/Al2O3 composites which were produced by melt compounding in Brabender mixer is characterized by light transmittance, haze, and clarity. Haze is the degree to which the specimen reduces the apparent contrast of the object.

The results show that the optical properties of polymer composites are strongly affected by particle content, particle size, and especially by difference in refractive indices between

polymer matrix and particles. It is also revealed that the light transmittance and haze of composites are mainly affected by difference in refractive indices, whereas the clarity is more affected by particle size. PMMA/SiO2 nanocomposites exhibit the best optical properties in all investigated composites because of a perfect index-matching. PC/SiO2 composites show decreased transparency caused by thermal degradation during mixing process and large difference of refractive indices.

PS/Al2O3 composites show better results of total light transmittance and haze than PS/SiO2 composites because of better index-matching, but lower clarity because of larger alumina agglomerates.

The haze value of all composites increases with increasing particle concentration because of increasing light loss via reflection and scattering. It is noted that the haze value of PMMA composites increases only slightly because of perfect index-matching, whereas the other composites show a drastic increase in haze.

Second, the main reason for increasing haze is Rayleigh light scattering in composites caused by dispersed particles, which sizes are smaller than the light wavelength used (a condition for Rayleigh scattering) [79]. According to SEM analysis, the average size of alumina particles (>10 lm) is much larger than the light wavelength used (589 nm), whereas the aver- age size of silica nanoparticles (about 80 nm) is much smaller than the light wavelength used. There- fore, the Rayleigh scattering in PS/Al2O3 composites is much weaker than that in PS/SiO2 composites. In the case of PC/SiO2 composites, the haze values are obviously increased compared to the other composites because of thermal degradation of PC matrix and large fluctuation of refractive indices.

The outer surfaces of respective samples are smooth with an average surface roughness below 1 μm, indicated by surface analysis in this work. It is known that surface roughness on the 100-lm size range is responsible for a loss in transparency, whereas surface roughness in the submicron range does not affect the transparency [80].

Chapter 2: Materials and Experimental Methods

In this chapter, raw materials and characterization techniques will be presented; moreover, the data on the samples will be presented in the table below. Sample A, B, D, E, G, H, and I were analyzed in two separate conditions: The use of the transparent ones can be in cases like cluster, radio, and display, while the black interior is used in applications like dashboard, doors, and seats. The two sample examples, 3 & 4, were used for radio display inside segment A and B. And the G250, A250, and T400 only came in black version for use in research.

I didn't bring up the part about segment for other optical surfaces, as those surfaces were under examination for the future (*).

OPTICAL SURFACE	*Substrate*	*Optical finishing*	*Segment*
Sample A	*PC*	*Matt*	*
Sample B	*PC*	*Matt*	*
Sample D	*PC*	*Matt*	*
Sample E	*PC*	*Gloss*	*
Sample G	*PC*	*Matt*	*D*
Sample H	*PC/PMMA laminated*	*Gloss*	*
Sample I	*PC/PMMA laminated*	*Gloss*	*
Type 3	*PC*	*Anti Glare*	*A & B*
Type4	*PC*	*Anti Glare*	*B*
G250	*PC*	*High gloss*	*
A250	*PC*	*Anti Glare*	*
T400	*PC*	*Matt*	*

2.1. Characterization Techniques

2.1.1. Spectral irradiance measurement (ILT-950)

For measuring light there are different products include radiometers, photometers, optometers, dataloggers, lux meters, chroma meters, spectrometers and spectroradiometers.

These meters are designed to measure light in the IR, NIR, VIS and UV Range. ILT950 remote optic irradiance spectroradiometer system can detect spectral range from 250 to 1050 nm.

Spectroradiometer system including integrated spheres, cosine correcting diffusers, fiber patch cords and our complimentary Spectrilight III software for easy and accurate measurement of spectral irradiance, as well as other parameters such as photometry, color coordinates, CCT, illumination, peak wavelength and more can be measured.

Combining high performance, precision, ease of use and a wide range of features, all in a robust, compact, portable design. The excellent performance of the ILT950 spectroradiometer was further enhanced by the addition of a new technologically advanced CMOS linear image sensor. The new sensor offers a more balanced overall spectral sensitivity (consistent in UV and lower in VIS and NIR), a faster response time, faster data transfer rates, and has a broader range of integration times, (30 µs to 59 s) which increases the overall dynamic range. The ILT950 spectroradiometer light measurement systems, come in two models for broad band, covering 200-1100 nm and UV 200-450 nm. ILT systems come complete with fiber optics, input optics, calibration and ILT's powerful SpectriLight III software.

2.1.2. Illuminance measurement (Konica Minolta CL-200A)

If you need to evaluate light illumination at a specific location or perform lux measurements, the T-10A is the illuminance meter of your choice. This advanced lux meter will quickly display the illumination and average measurement values on the LCD screen. You can easily compare the illuminance values and display them in either a percentage or a difference value.

Programming the T-10A is easy; you can enter the target level by taking actual measurements, or you can enter the level by typing it on the handy keypad. The high versatility of this instrument enables the measurement of both intermittent and continuous light sources, and the unit automatically calibrates the instant when it is switched on. Even first-time users find it easy to input color correction factors that can be used to measure any specific light source.

T-10A is one of the most useful and functional lux meters on the market today. Due to the expansive range of measurements from 0.01 to 299,000 lx and the ability to switch ranges automatically, this instrument provides extremely accurate results for tasks involving the measurement of pulse width modification of controlled light sources. If you measure multiple sources, you can easily remove the head of the receiver instruments to simplify this process.

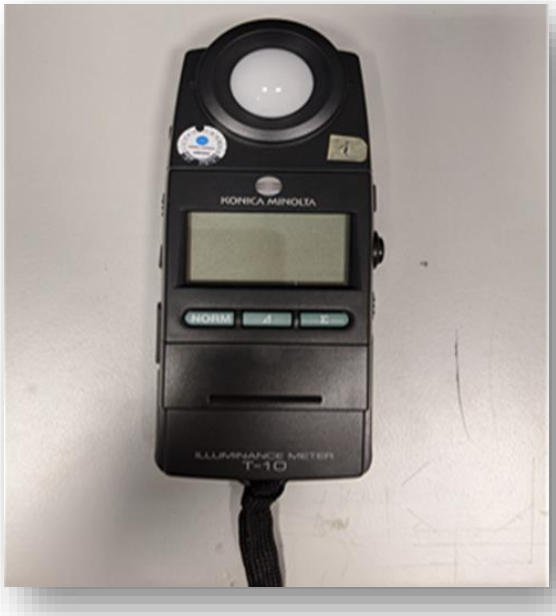

2.1.3. Spectrophotometer

The principle of spectroscopic analysis is based on passing the light of a known wavelength through a sample and measuring how much light is absorbed or reflected. Therefore, the spectrophotometer must be able to generate discreet wavelengths of light and pass them through the sample.

In addition to the previous process, spectrophotometers function by reflecting light from the surface and recording the wavelength distribution of the reflected light. The sample is illuminated by a polychromatic light source and the reflected light is recorded as spectral data by a detector. The values can be calculated and converted from the spectral data to a number of three-dimensional color spaces. The data presented in this work is provided in the color space of CIE L*a*b* to ensure that it has occurred.

Specular reflection happens when light reflects at the equal but opposite angle from the light source, this reflection occurs strongly on objects with glossy smooth surfaces. When the reflected light is scattered in many directions, it is called diffuse reflection and this reflection occurs strongly on objects with matt or irregular surface.

To measure an object true color, without the influence of surface conditions, the use of Specular Component Included (SCI) measurement mode is preferred. SCI mode includes both the specular and diffused reflected light and is ideal for computer color matching and monitoring color quality.

Specular Component Excluded (SCE) measurement mode, which excludes specular reflected light, is used to evaluate color of an object which correlates to visual perception. Using SCE mode, a glossy surface will typically measure darker than a matt surface of the same color; similar to how our eyes see it. This mode is typically used during quality control evaluations to ensure color matches the color standards by visual inspection.

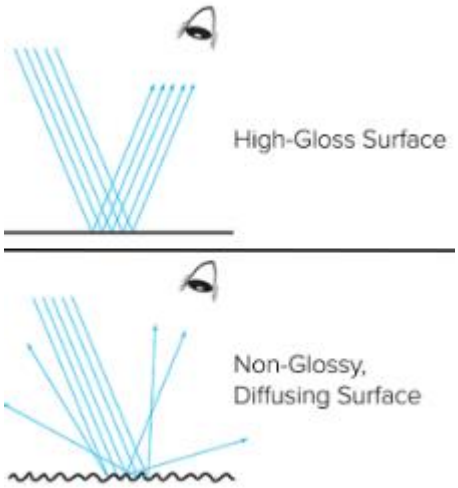

2.1.4. Spectrophotometer KONICA MINOLTA CM-3610A

The CM-3610A Spectrophotometer is a high-precision and high-reliability bench-top instrument with vertical alignment capable to measure colors either in reflectance (diffused illumination, 8-degree viewing) or transmittance (diffused illumination, 0-degree viewing), the detector is Silicon photodiode array and spectral separation device is diffraction grating and wavelength range is between 360 to 740 nm. which reflectance mode can be useful for black sample and transmittance mode for transparent ones. And for calculating color changes due to weathering, the Spectra Magic software tried to use SCE for all parameter (L, a, b).

Light from the pulsed xenon lamps are diffused by reflection from the inner surface of the integrating sphere and the surface of the white calibration plate covering the reflectance measurement aperture, and finally illuminate the specimen in the transmittance chamber and the light transmitted by the specimen is received by the specimen- measuring optical system and guided to the sensor, then the light from the specimen-measuring optical fiber and from the illumination-monitoring optical fiber is divided into each wavelength component and projected onto the sensor array section, which convert the light into proportional currents and output the currents to the analog processing circuit.

By using CM-3610A calculating the Haze(D1003-97) (A) is really easy, and haze has been estimated by transmittance mode for all transparent samples. When the White Calibration Plate is positioned over the reflectance measuring aperture, the measurement geometry for transmittance measurements becomes di:0°. Haze thus offering a wide range of applications such as Plastics, Textiles, Paints, Ceramics etc.

Using this Optical System technology can handle measurements for numerical gloss control (NGC) for simultaneous measurements with specular component included (SCI) and specular component excluded (SCE). Additionally, numerical UV control (NUVC) is the top technology for UV adjustments to measure samples containing optical brighteners like paper textiles, pulp or other chemicals.

These technologies ensure the repeatability and highest accuracy levels. With a reduced number of moving parts, the CM-3610A has superior reliability and offers an incredible price performance ratio.

Spectra Magic is a color measurement software package that can be used to interface with Konica Minolta instruments and provide extended reporting and analysis of color and color difference. The CM-3610A can measure both the reflectance of opaque objects and the transmittance of transparent or translucent solid materials such as plastics.

2.1.5. Varian spectrophotometer Cary 500 UV-Vis-NIR

Spectral photometry is a device for measuring the intensity of wavelength specific to each color. Spectrometers disperse light in various wavelengths using dispersive elements such as gratings (diffractive elements). The dispersed light is then detected by image sensors and other devices.

The Cary 500 enables you to independently control the parameters in the UV-Vis and NIR regions so you don't have to compromise when scanning across the whole range. For example, if you want more detail in the NIR without sacrificing measurement time, just set a narrow SBW and small data interval in the NIR and a wider SBW and larger data interval (and thus a faster scan speed) in the UV-Vis. In UV-Vis NIR spectrophotometry, this is a measure of the amount of light that is selectively absorbed by molecules within a substance. The absorption in the sample is dependent on the distance that the light travel through the sample. It also dependent on the wavelength of the incident light as various combination of molecules will absorb different wavelength. The resulting peaks from the various absorption peaks allow characterization and quantitative analysis of sample.

With this instrument we measured the HAZE of our samples which is tell us the percentage of the scattered light that was transmitted, in the middle of visible range at 550 nm.

2.1.6. Veeco DEKTAK 150 Profilometer

The Dektak 150 from Veeco is a surface profilometer that takes Two-dimensional surface profile measurement. with using contact profilometry techniques. The Dektak 150 uses stylus which Stylus has Low Inertia Sensor. A sharp probe tip is scanned across a material in a linear fashion to create a line profile of height vs distance. we can use it for surface topography measurements, roughness, and step heights.

The Dektak 150 can be equipped with a 150-millimeter X-Y auto stage that provides 3D mapping, automation and programmability of over 200 sample sites. It also can be configured with a 6-inch square, porous chuck for photovoltaic applications. The innovative design of the Dektak 150 accommodates samples up to 90 millimeters thick, performs long scans of 55 millimeters, and provides a larger X-Y translation than competing systems.

With 4-angstrom step-height repeatability using optional ultra-low-noise electronics, the Dektak 150 option provides the flexibility to perform precise step-height measurements for thin films down to 10 angstroms, as well as thick-film measurements up to several hundred microns thick. The Low-Inertia Sensor 3 (LIS 3) head incorporates key technology advances to deliver extremely accurate measurements with unprecedented sensitivity.

The system's 1-millimeter standard vertical range coupled with up to 120,000 data points per scan deliver exceptional capability. The result of all these features is exceptional horizontal and vertical resolution, enabling precise planarity scans for measuring radius of curvature, flatness, and waviness, as well as characterizing thin-film stress on wafers.

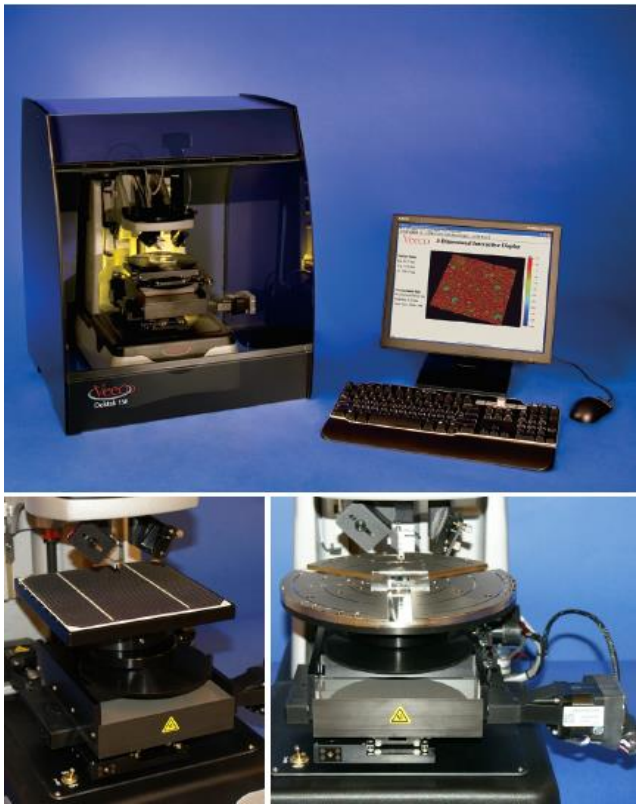

2.1.7. Gloss meter

The Rhopoint IQ quantifies surface quality problems that are invisible to a standard glossmeter and profiles how light is reflected from a surface. This incredibly advanced instrument measures: 20/60° Gloss, Haze, Reflected image quality (RIQ), Distinctness of image (DOI).

The Rhopoint IQ is different to a gloss meter as it uses a linear diode array (LDA) at 20° to measure the distribution of reflected light between 12.75°–27.25°. The instrument does not have physical receiver apertures like a conventional gloss meter; the 20° gloss value is obtained by measuring with the elements of the linear array that correspond to the angles specified in the standards. Conventional glossmeter optics are used at 60° & 85° and these fully comply with international gloss standards such as ISO 2813 and ASTM 523. On the surface, we can see gloss unit for 20° and 60°, if the quantity of gloss unit is more than 70 we have to consider gloss unit of 20°.

2.1.8. Confocal Microscope

Confocal microscope is a useful tool for characterizing nanoscale surface deformation in the early stages of physical degradation. The Leica DCM8 unites the advantages of HD confocal microscopy and interferometry with a wealth of additional features that facilitate the accurate and reproducible characterization of multiple material surfaces. At the touch of a button, the sample is scanned vertically so that every point on the surface passes through the focus. Within seconds the Leica DCM8 acquires multiple confocal images at different vertical points along the objective's depth of focus, automatically adjusting illumination if required. Out of focus information is then eliminated and a detailed profile of the surface topography generated.

With Leica DCM8 we can obtain HD Imaging, HD 3D Topography, Profiles, Coordinates, Thickness, Roughness, Volume, Surface Texture, Spectral Analysis, Color Analysis. Illumination is done by LED light sources: red (630 nm), green (530 nm), blue (460 nm) and white. Simple image is captured with brightfield and darkfield with high lateral resolution.

Chapter 3: Results and Discussion

In this chapter, the optical, physical and topographical characteristics of the samples will be discussed.

3.1. Solar Exposure Measurements

In this study I compared weather data of Florida site and Genova such as temperature, humidity, solar radiation, UV radiation and leaf wetness which are the influencing parameter in natural weathering. All the data originally were measured on daily basis but for facilitating of analysis, I used the monthly average. The ratio of weathering parameters between these two cities is a simple indicator that shows how these parameters are similar. The more this ratio is close to 1 the more they are similar.

The UV radiation ratio of Genova to Florida is $UV_{Genova}/UV_{Florida}=0.88$

The Solar radiation ratio of Genova to Florida is $SR_{Genova}/SR_{Florida}=0.79$

The Leaf wetness ratio of Genova to Florida is $LW_{Genova}/LW_{Florida}=0.41$

The average temperature of Florida in the first five months and in the last three months of the year is about 10°C more than Genova while in June, July and August the difference is less than 5°C. The maximum difference of average humidity is about 33% in January, and the minimum difference is in November around 5%.

3.2. Irradiance

In this analysis I present the measurement of spectral irradiance and illuminance for three different segments (A-B-D). Two objectives have been followed, the first objective was to compare spectral irradiance of sunlight inside the car with filter spectrum which is commonly used for testing aging of the internal components and the second goal was the assessment of the relative illuminance between some internal components with considering the different orientation and the different position inside the car.

For measuring Spectral of irradiance, the calibrated ILT-950 spectroradiometer has been utilized for measuring of “segment A” on 21st June 2018 inside the car with close windows at three different times. As it can be seen, different spectral of irradiance is due to the clear weather condition.

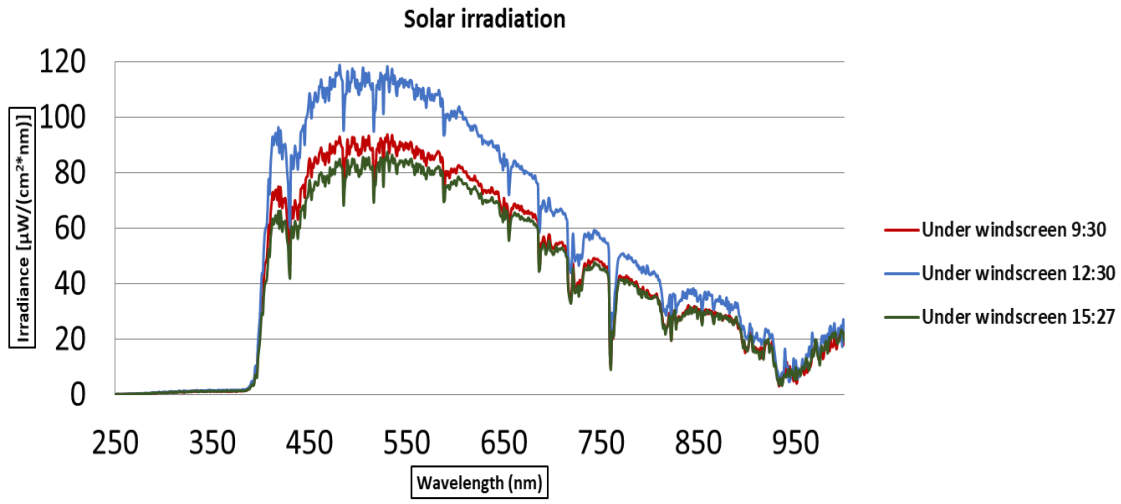

For "segment B" the measurements were performed inside the car with close windows at three different times on 19th June 2020. As you can see in the graph again the different spectral of irradiance is refer to the clear weather condition.

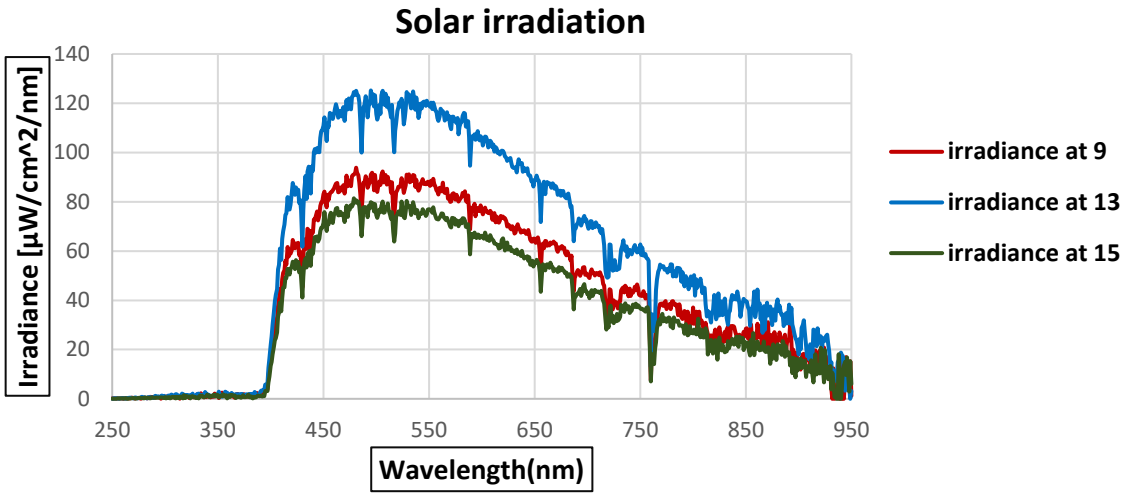

The measurement of the spectral irradiance for "segment D" was carried out on 5th June 2020 at three different time with close windows. Overlapping of the irradiance at 9 AM and 13 PM is due to the cloudy weather condition.

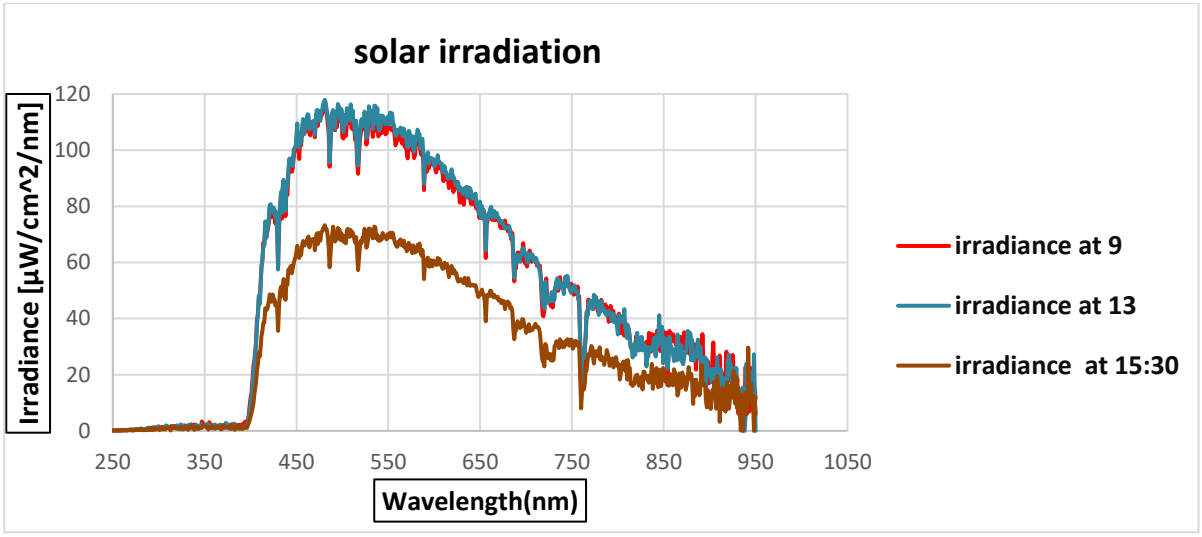

3.3. Illuminance Measurement

Illuminance was measured with Konica Minolta CL-200A, this advanced lux meter will quickly show on the LCD screen the illumination and average values of measurements. You can easily compare illuminance values and have them shown either in a percentage or a difference value. Our measurement was made at three different times and four car orientation on the 14 different surfaces. Four car orientation is, North-East, South-East, South-West, North-West.

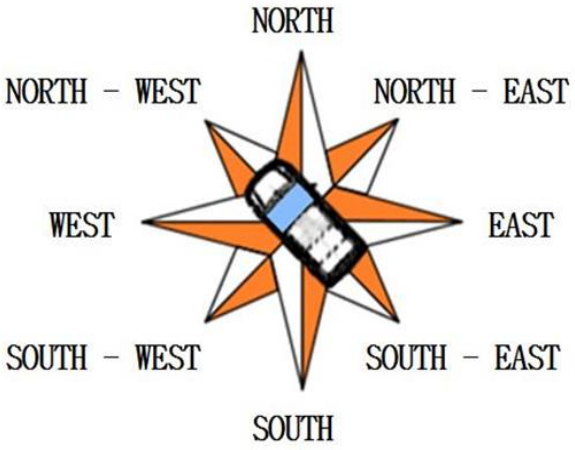

For calculating the luminous flux that every single surface at different segment received we tried to collect Lux at three different time in the same day, and at each determined time I tried to put the car in the four different orientation, then make and average from the amount of lux that every surface received. For analyzing the degradation of the interior part of vehicles, and also for stimulating the natural weathering in accelerated environment knowing the amount of Lux is important. In the following graph I will show the quantity of illuminance for "segment D" that was collected in the partly cloudy day on 5th June 2020. You can observe the amount of irradiance (w/m2) at different time in the graph, that you can find in the "Atmospheric Physics Meteorological Station" website of Department of Physics, University of Turin.

The data on illumination for segment A and B has been listed in the appendix

Segment D				Dashboard	Top left door	Top right door	Parcel shelf	Gear shift	Tunnel	Radio	Right seat	Left seat	DAB	Rear seat	Center right door	Center left door	Cluster
Time	Climate condition	Irradiance W/m2	Car orientation	Illuminance(lux)													
9:00	partly cloudy	600	SW	54600	44700	3760	56900	513	1860	26900	3990	2320	3420	51500	1923	1732	1728
9:00	partly cloudy	600	NW	46900	25500	39100	60700	2610	1860	2014	1366	879	2430	1663	1724	1262	1136
10:04	partly cloudy	826	NE	63100	4750	42900	56900	54600	3360	5410	2937	2315	2075	45800	1610	3250	1506
11:00	partly cloudy	578	SE	65400	43500	39100	52100	4980	5570	1964	4320	3190	2111	882	2791	2914	800
11:45	partly cloudy	501															
12:57	partly cloudy	428	SW	71500	49600	46100	74500	69400	3260	3250	48200	62000	6770	1336	3930	1820	1199
12:57	partly cloudy	428	NW	85700	65500	6470	81600	79500	1234	19350	2418	67500	29100	1190	1820	2148	1855
13:25	partly cloudy	925	NE	83200	52800	58000	81300	4400	1466	2004	2720	1184	1643	819	8090	8550	945
14:08	partly cloudy	862	SE	81500	4200	63400	77000	79300	2085	1180	68000	2157	27500	649	2066	1835	1132
15:18	partly cloudy	724	SW	59000	3930	45000	48700	56100	36800	2136	2920	43100	1862	683	1711	36400	1027
15:18	partly cloudy	724	NW	57200	44300	3850	46600	55500	53800	1442	44100	27600	1565	962	35500	1372	645
15:18	partly cloudy	724	NE	49100	39200	2735	55200	2813	1168	1297	749	1280	45600	1290	825	1675	29500
15:56	partly cloudy	642	SE	54300	3050	41300	56200	2820	1184	1793	1743	863	1052	573	1258	1187	491

Time	Irradiance W/m2	Dashboard	Top left door	Top right door	Parcel shelf	Gear shift	Tunnel	Radio	Right seat	Left seat	DAB	Rear seat	Center right door	Center left door	Cluster
09:00	600	57500	29613	31215	56650	15676	3163	9072	3153	2176	2509	24961	2012	2290	1293
13:00	428	80475	43025	43493	78600	58150	2011	6446	30335	33210	16253	999	3977	3588	1283
15:30	724	54900	22620	23221	51675	29308	23238	1667	12378	18211	12520	877	9824	10159	7916

Figure 3.1. Average illuminance between four different car orientation (SW-NW-NE-SE) at three different time for each surface

As it can be seen for "segment D", dashboard, parcel shelf and gear shift have higher average daylight illuminance and center left door, center right door and cluster have lower average daylight illuminance.

In the following for "segment A", dashboard, top of the doors and parcel shelf has higher average daylight illuminance and center of the doors and cluster has lower average daylight illuminance.

For "segment B" dashboard and top of the doors has higher average daylight illuminance and DAB radio and cluster has lower average daylight illuminance.

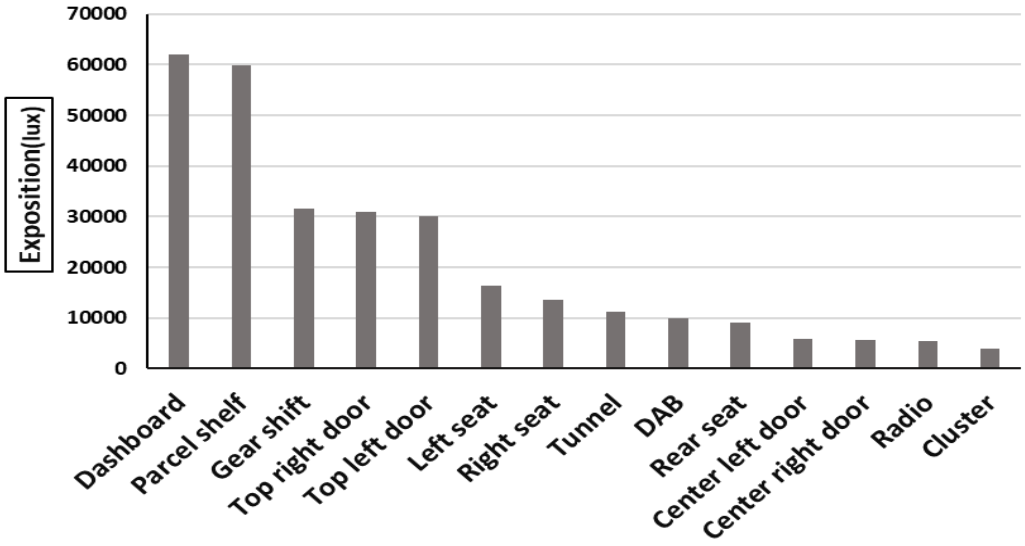

Figure 3.2. Average daylight illuminance weighted to irradiance (lux)-Segment D

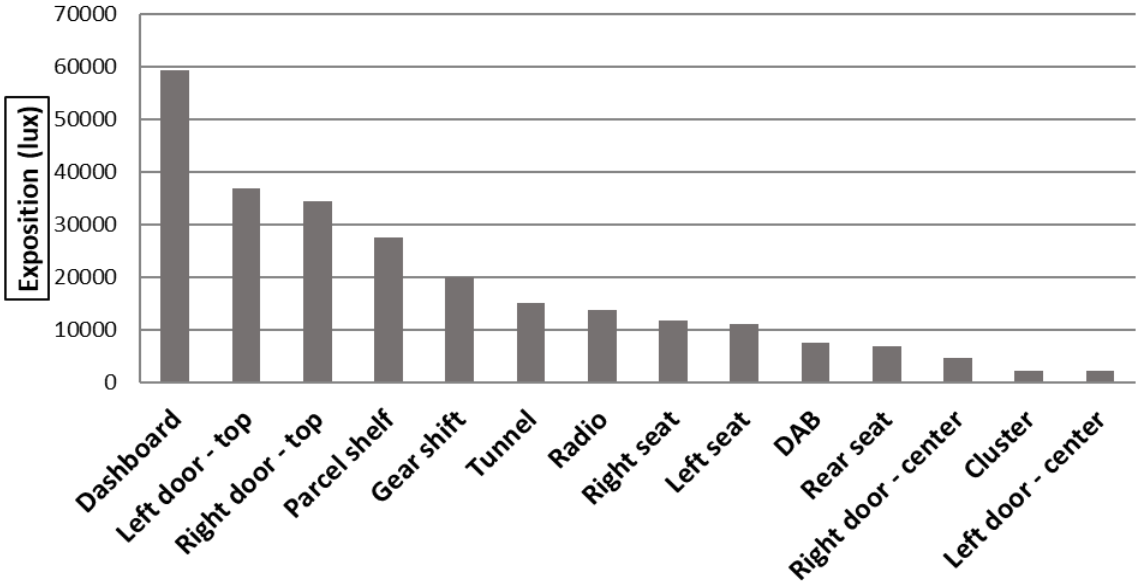

Figure 3.3. Average daylight illuminance weighted to irradiance (lux)-Segment A

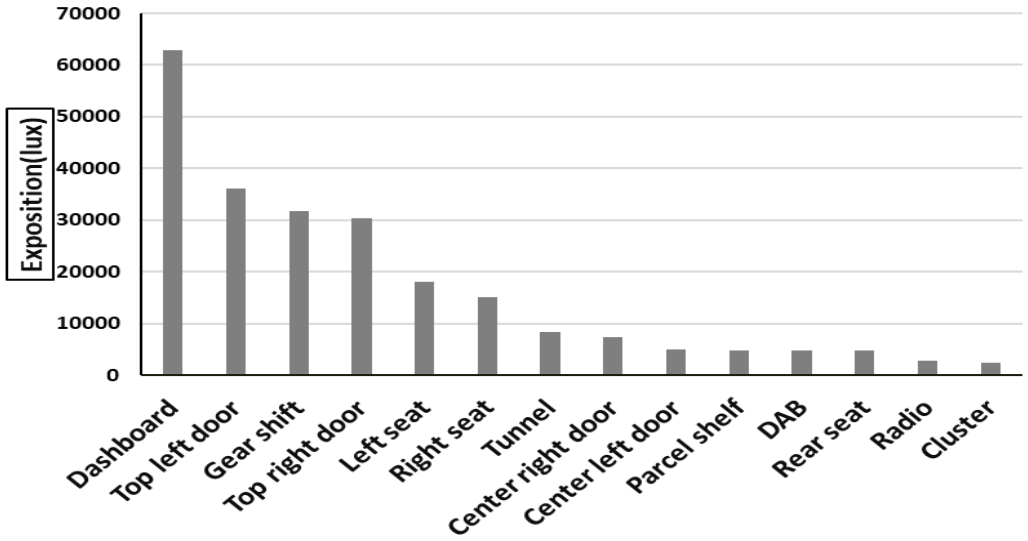

Figure 3.4. Average daylight illuminance weighted to irradiance (lux)-Segment B

Illuminance analysis of Segment D

Regarding to previous table you understood that different interior part of car receives different illuminance during the day or even the same surface in the different orientation takes diverse amount. In the picture of segment D, we try to show the quantity of Lux by different colors.

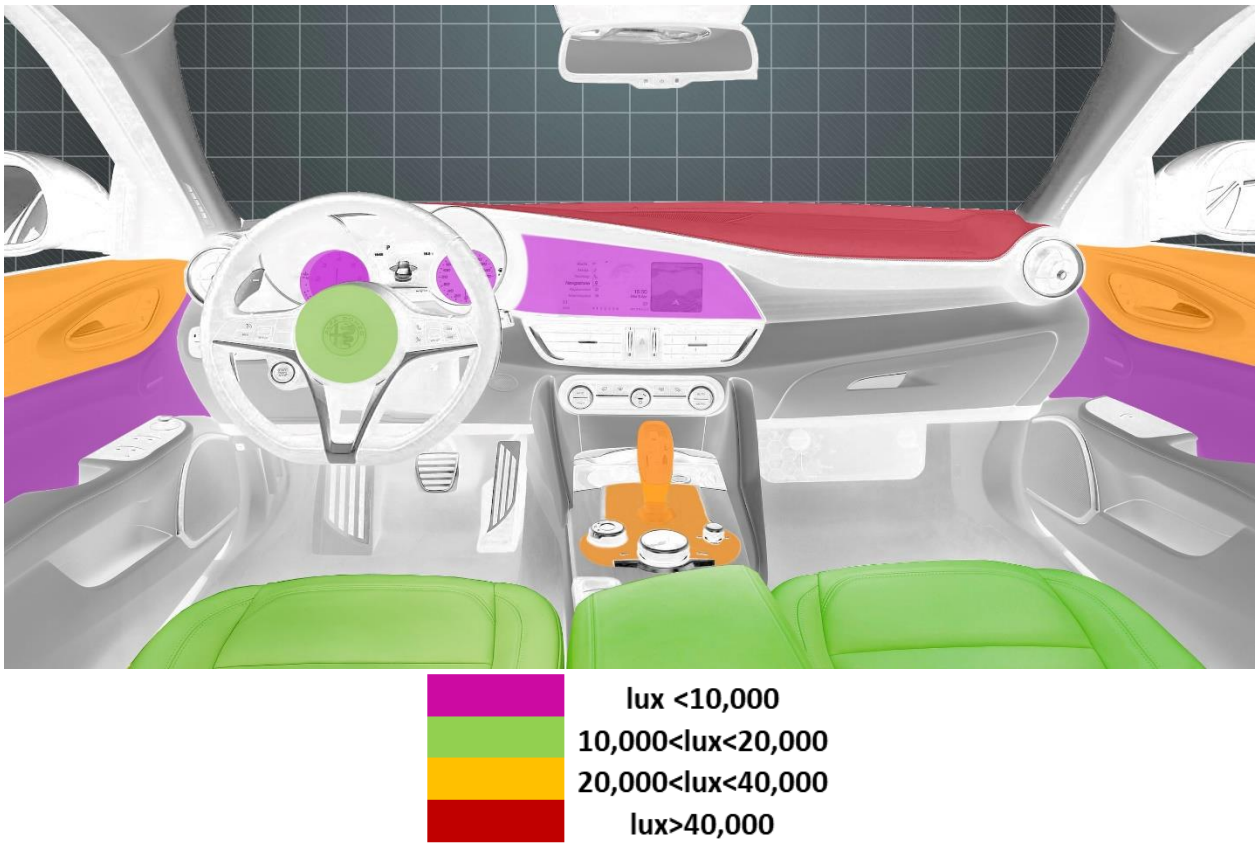

Average daylight illuminance weighted to irradiance (lux) – Segment D		
Surface	Exposition (lux)	Ratio respect dashboard (%)
Dashboard	62038	100
Parcel shelf	59956	97
Gear shift	31685	51
Top right door	30911	50
Top left door	29999	48
Left seat	16384	26
Right seat	13605	22
Tunnel	11177	18
DAB	10003	16
Rear seat	9155	15
Center left door	5859	9
Center right door	5720	9
Radio	5370	9
Cluster	4027	6

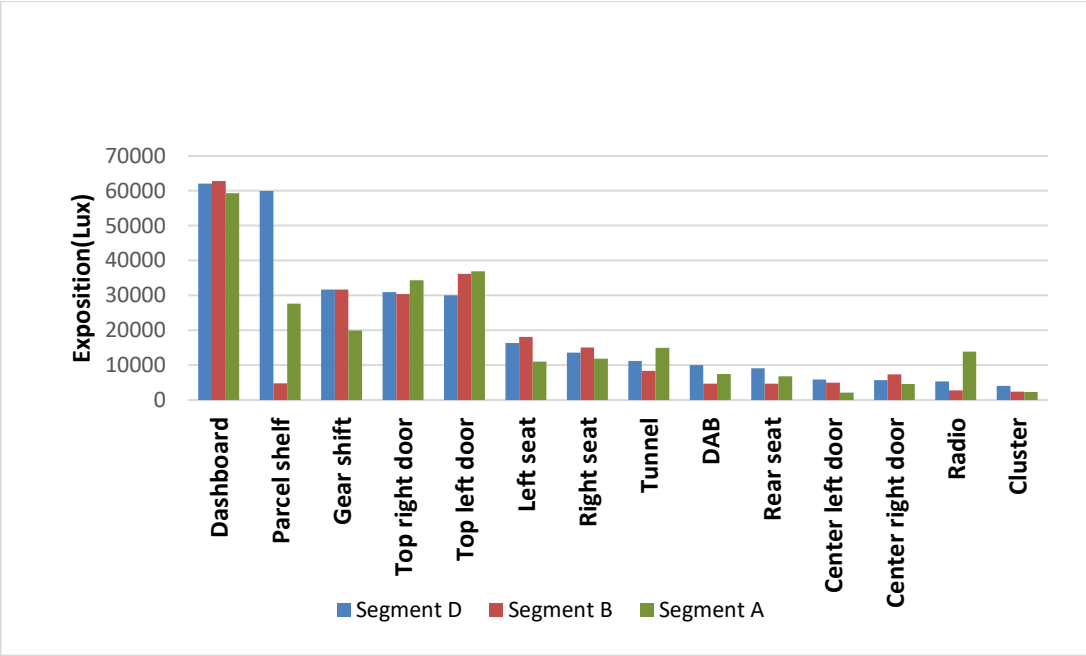

Figure 3.5. Comparison of Average daylight illuminance weighted to irradiance for 3 segments

With comparison of average daylight illuminance weighted to irradiance between 3 cars:

- Segment D receives more than segment A in most of the surfaces except, top of the doors, tunnel and radio
- Segment D receives more than Segment B in different surfaces except right seat, left seat, top left door and center right door, and they receive almost the same exposure in dashboard and Gear shift
- The ratio between the lowest (cluster) and the highest illuminance value (horizontal dashboard) in segment D is 6% and in the segment A and B is 4%.

3.4. Optical and Physical Characterization

3.4.1. Transparent Samples

During this survey one of the main goals was analyzing the optical characterization of our samples after natural and artificial weathering. Most of the samples that we observed after the weathering, the substrate was polycarbonate or polycarbonate/poly methyl methacrylate in the form of transparent or black one with the high gloss finishing or matt finishing. These optical surfaces are used mostly in the infotainment, cluster, and cookpit.

Color Measurement

In the table below you can find our different optical transparent surfaces with the detail of finishing which was under the accelerated weathering by the Standard SAE J2412. We are going to find out how it is going to change the color and haze of our transparent sample when they are under the specified irradiance exposure at 600kj, 900kj, and 1240kj respect to the reference sample without any exposure.

			Delta E		
Optical surface	Substrate	Optical finishing	600KJ	900KJ	1240KJ
Sample A	PC	Matt	1.52	11.5	8.35
Sample B	PC	Matt	1.51	10.98	8.78
Sample D	PC	Matt	2.53	2.36	3.67
Sample E	PC	Gloss	2.24	2.74	3.2
Sample G	PC	Matt	1.39	2.18	4.41
Sample H	PC/PMMA laminated	Gloss	1.17	1	0.68
Sample I	PC/PMMA laminated	Gloss	1.1	0.99	0.61

The following graph shows us a significantly increase in sample A and B, which this result is not acceptable, we need more parameter for analyzing the behavior of those samples. As defined in the standard, the changes of color (ΔE) less than 3 is the suitable outcome, therefore for sample D, E and G the rate of increasing is suitable. Finally, for sample H and I the rate of changes is less than 3.

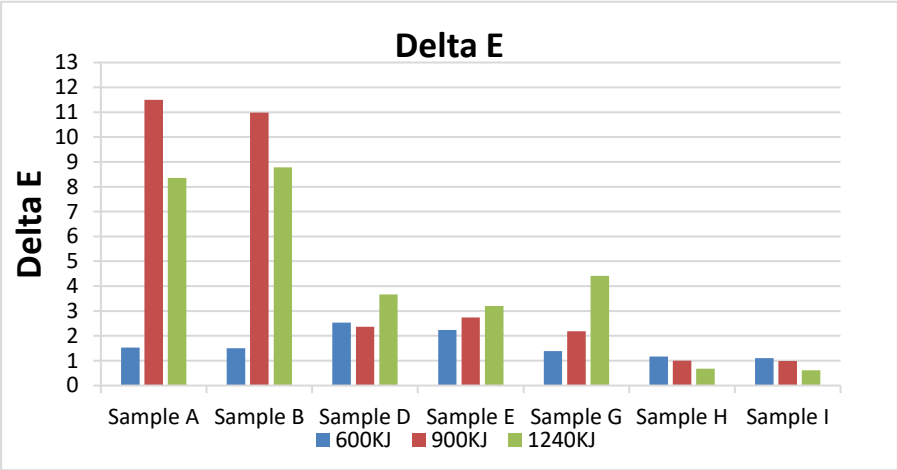

Haze Measurement

Haze is another important optical parameter for studying our transparent samples after weathering, which will show us the amount of scattered light respect to incident light. As we predicted and shown in the figure, all samples showed the output of the uptrend.

	Haze			
SAMPLE	reference	600KJ	900KJ	1240KJ
Sample A	0.66	0.98	6.03	10.51
Sample B	0.53	1.90	7.69	8.32
Sample D	0.43	0.58	1.19	1.07
Sample E	0.57	0.79	1.19	1.41
Sample G	0.59	0.59	1.40	4.22
Sample H	0.38	0.55	2.00	4.54
Sample I	0.32	0.59	2.17	6.17

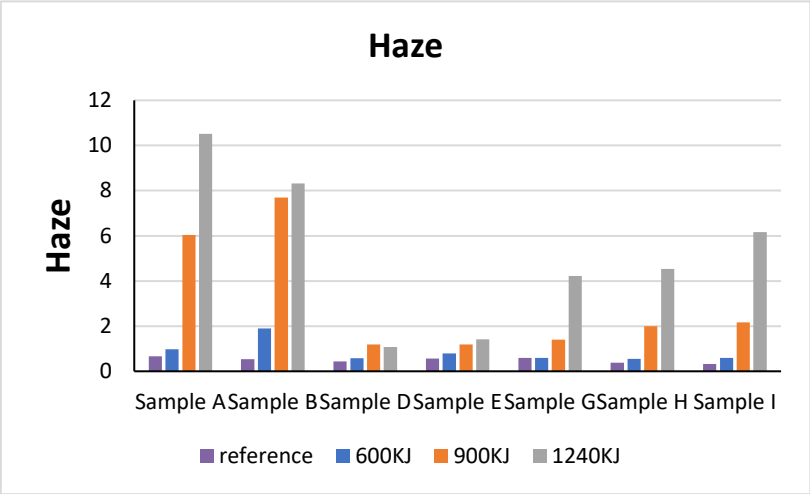

Roughness

The following plot will demonstrate the roughness for our transparent samples which was made by profilometer Vecco Dektak150. In the case of sample A and B the amount of roughness at reference and after weathering at 600kj is mostly equal. This means that the surface of our samples during accelerated weathering up to 600kj doesn't have any major changes. This small change in roughness before and after weathering could be confirm by the appearance of the samples, which means that even the eyes cannot see the damage on the surface. But with more doses of irradiance at 900 kj and 1240 kj, you will see an increase in roughness.

In the case of sample G and H you can see the same trend for both of them. After 600 kj of exposure to the surface of the sample, the increase in roughness is clear, but in the next steep at 900 kj we find a slight decrease in roughness, which is not an impressive amount. I can say that after 600 kj and 900 kj the roughness is more or less the same. It means more or less the same actions at 600kj and at 900kj. Finally, under the 1240 kj exposure the amount of roughness is bigger than others.

For sample I, the strange result for the roughness of the reference was higher than 600kj and 900kj, although all the measurements are in the micrometer unit and, in general, the difference between the reference and 600kj and 900kj is not so huge but we didn't expect that. In the last step at 1240 kj, the roughness is greater than the previous one.

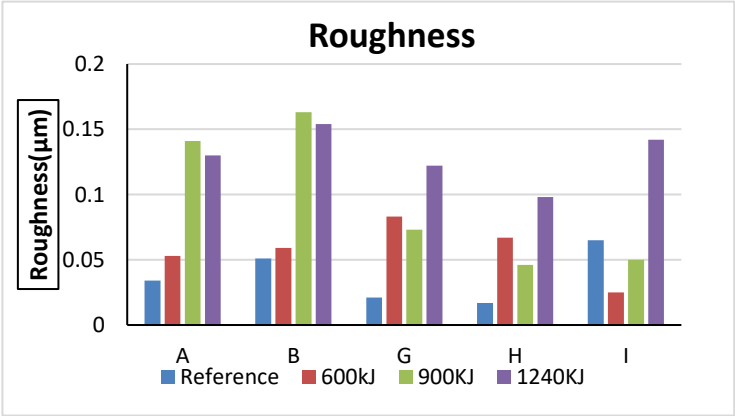

	Roughness(µm)			
Sample	**Reference**	**600kJ**	**900KJ**	**1240KJ**
A	**0.034**	**0.053**	**0.141**	**0.13**
B	**0.051**	**0.059**	**0.163**	**0.154**
G	**0.021**	**0.083**	**0.073**	**0.122**
H	**0.017**	**0.067**	**0.046**	**0.098**
I	**0.065**	**0.025**	**0.05**	**0.142**

3.4.2. Black Samples

A modern car is a large assemblage of parts made of a variety of materials. Many of these parts have a protective coating applied to improve the appearance or provide additional durability of the substrate. In many coating systems, the uppermost layer is a clear coating (5–50 µm in thickness), Not only does it protect the underlying layers or substrate from chemical and UV degradation, but it also protects against mechanical damage that may result in surface scratches. Consumers want a permanent, scratch-free finish on all parts of their vehicles, which shows that scratch performance is becoming the highest customer concern for automotive paint systems [81].

We analyzed the color measurement and the haze of our transparent sample, which can be used in cluster and display. In other interior parts of the car, such as gear shifts, dashboard, DAB and doors, we can't use transparent ones, so we're going to paint a black on substrate. In this condition, it is better to measure the Gloss of our sample in order to understand how the surface of the samples is aged after weathering. In all cases, the measurement was averaged for 5 replicates of the specimen.

			Gloss			
Optical surface	**Substrate**	**Optical finishing**	**R**	**600 KJ**	**900 KJ**	**1240 KJ**
Sample A	**PC**	**Matt**	**85.7**	**86.1**	**82.5**	**72.9**
Sample B	**PC**	**Matt**	**85.4**	**84**	**84.6**	**67.6**
Sample D	**PC**	**Matt**	**79.7**	**69.78**	**49.5**	
Sample E	**PC**	**Gloss**	**80.2**	**72.08**	**59.74**	
Sample G	**PC**	**Matt**	**85.7**	**81.8**	**45.8**	**44.1**
Sample H	**PC/PMMA laminated**	**Gloss**	**84.7**	**87.9**	**85.6**	**79.8**
Sample I	**PC/PMMA laminated**	**Gloss**	**86.8**	**87.8**	**85.4**	**82.9**

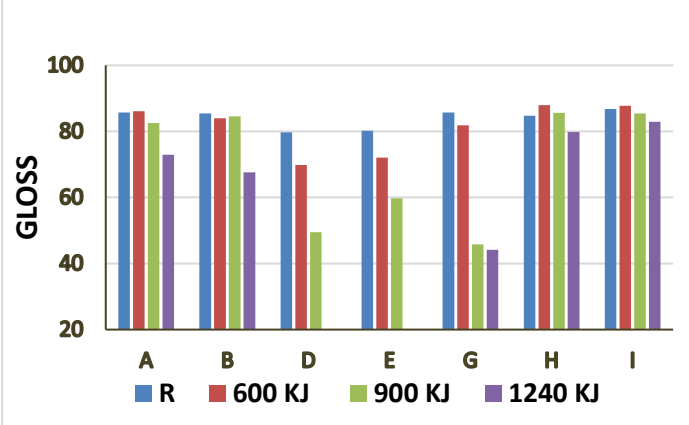

For better understanding the deviation of gloss, we are going to show the variation respect to the reference sample. Unfortunately, we did not measure gloss for samples D and E at 1240 kj because they were damaged.

	ΔGU/GUTQ (%)		
Sample	**600 KJ**	**900 KJ**	**1240 KJ**
A	**0.47**	**3.76**	**15**
B	**1.64**	**0.91**	**20.79**
D	**12.4**	**37.9**	**!**
E	**10.1**	**25.5**	**!**
G	**4.5**	**46.5**	**48.5**
H	**3.71**	**1.02**	**5.83**
I	**1.08**	**1.68**	**1.56**

Roughness

In this section, we would like to know the correlation of roughness of our samples with all optical parameters (color measurement and gloss) and, far along in particular, the relationship between roughness and all field parameters (Sa, Sq, Ssk, Sku), more over with these areal field parameters we will see how the topographic of our sample has changed. Because of this important issue, we have tried to measure the roughness of the surface three times and then make the average.

After analysing our numbers and reviewing our topographic images, which were extracted by a confocal microscope (Leica DCM8), we decided to measure again for samples A and B, and finally, by using a microroughness filter, we achieved the brilliant and expected results.

With microroughness filter, this operator is used to separate the roughness and waviness of profile. The separation criterion is a wavelength threshold, called the cut off. The filter distributes the large wavelength to the waviness and the small wavelength to the roughness. The quality of the separation depends both on the type of filter and cut off value. This operator allows us to obtain the roughness and a waviness studiable which can be done individually.

In the first graph, we show the roughness of our sample before using a microroughness filter, and in the second graph, you can see the result after using a filter.

In this section, we would like to know the correlation of roughness of our samples with all optical parameters (color measurement and gloss) and, far along in particular, the relationship between roughness and all field parameters (Sa, Sq, Ssk, Sku), more over with these areal field parameters we will see how the topographic of our sample has changed. Because of this important issue, we have tried to measure the roughness of the surface three times and then make the average.

	Roughness(µm)			
Sample	R	600KJ	900KJ	1240KJ
Sample A	0.0733	0.0569	0.0870	0.0898
Sample B	0.1540	0.0765	0.1080	0.0646
Sample D	0.0196	0.0327	0.0351	0.0596
Sample E	0.0270	0.0234	0.0303	0.0256
Sample G	0.0200	0.0221	0.2239	0.1403
Sample H	0.0199	0.0215	0.0175	0.0335
Sample I	0.0769	0.0448	0.0413	0.0555

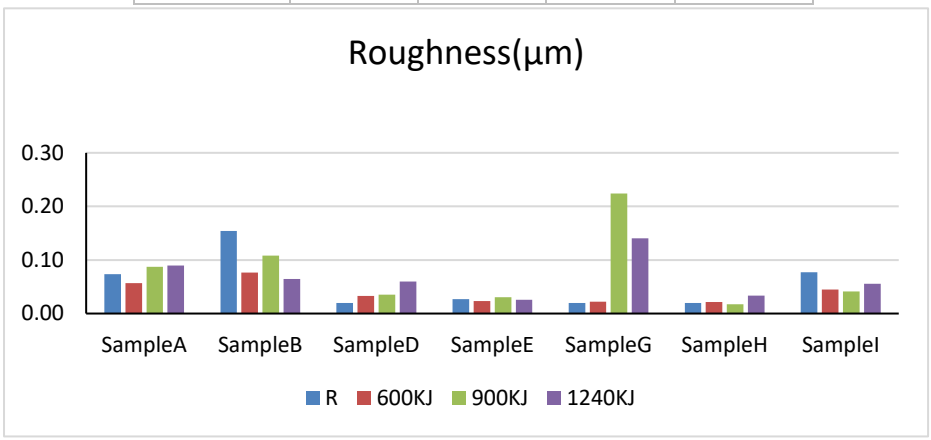

	Roughness(µm)			
Sample	R	600KJ	900KJ	1240KJ
Sample A	0.0182	0.0134	0.0214	0.0219
Sample B	0.0224	0.0162	0.0208	0.0299
Sample D	0.0179	0.0202	0.0231	0.0562
Sample E	0.0228	0.0210	0.0324	0.0513
Sample G	0.0136	0.0175	0.0542	0.0773
Sample H	0.0138	0.0141	0.0142	0.0412
Sample I	0.0173	0.0173	0.0200	0.0288

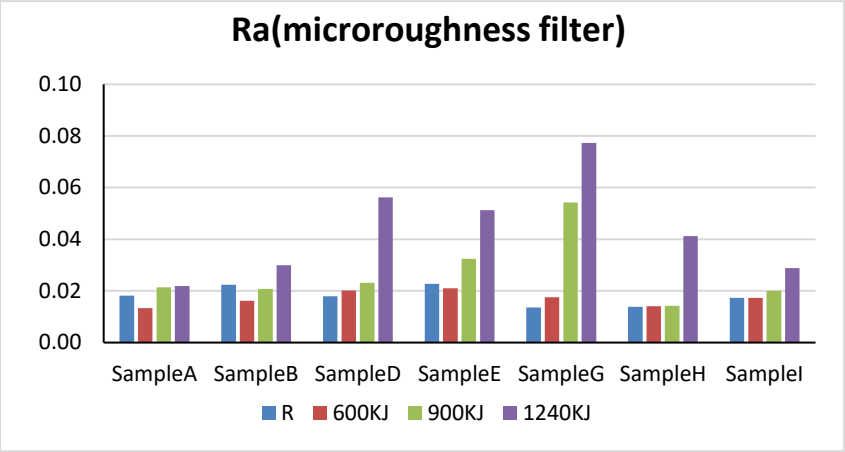
Ra(microroughness filter)
0.10
0.08
0.06
0.04
0.02
0.00
SampleA
SampleB
SampleD
SampleE
SampleG
SampleH
SampleI
R
600KJ
900KJ
1240KJ

Bibliography

1 . V Wong, K., & A Paddon, P. (2014). Nanotechnology impact on the automotive industry. Recent patents on nanotechnology, 8(3), 181-199.
2 . Shamsundara, B. V., Mannikar, A. V., & Shridhar, T. N. (2011). Study on Polymer Degradation due to Weathering and its Effect on Vehicle Safety (No. 2011-26-0097). SAE Technical Paper
3 . McGreer, M. (2003). Weathering testing guidebook. *Atlas Material Testing Technology*.
4 . Mayne, N. Plastics-A material choice in the automotive industries. *Association of plastics manufactures in Europe, Technical paper*
5 . Chandra, R., & Saini, R. (1990). New developments in the degradation, stabilization, and sensitization of poly (methyl methacrylate). *Journal of Macromolecular Science—Reviews in Macromolecular Chemistry and Physics*, *30*(2), 155-208
6 . Iannuzzi, G., Mattsson, B., & Rigdahl, M. (2013). Color changes due to thermal ageing and artificial weathering of pigmented and textured ABS. *Polymer Engineering & Science*, *53*(8), 1687-1695.
7 . *FORMULATION OF INDIA SPECIFIC WEATHERING CYCLE REQUIRED FOR POLYMER TEST*
8 . *NEW Q-FOG CRH CYCLIC CORROSION TESTER WITH RELATIVE HUMIDITY CONTRO*
9 . Zito, S., Castel, T., Richard, Y., Rega, M., & Bois, B. (2020). Optimization of a leaf wetness duration model. *Agricultural and Forest Meteorology*, *291*, 108087
10 . Gok, A., Ngendahimana, D. K., Fagerholm, C. L., French, R. H., Sun, J., & Bruckman, L. S. (2017). Predictive models of poly (ethylene-terephthalate) film degradation under multi-factor accelerated weathering exposures. *PloS one*, *12*(5), e0177614
11 . Krzymien, M. E. (1997, April). PVC photo-oxidative degradation: Identification of volatiles. In *Macromolecular Symposia* (Vol. 115, No. 1, pp. 27-40). Basel: Hüthig & Wepf Verlag
12 . Hollande, S., & Laurent, J. L. (1998). Weight loss during different weathering tests of industrial thermoplastic elastomer polyurethane-coated fabrics. *Polymer degradation and stability*, *62*(3), 501-505
13 . SAE, J. (1885). Accelerated Exposure of Automotive Interior Trim Components Using a Controlled Irradiance Water Cooled Xenon-Arc Apparatus, 1993 KJ/m2 irradiance, borosilicate filter. *Society of Automotive Engineers*
14 . Ram, A., Zilber, O., & Kenig, S. (1985). Life expectation of polycarbonate. *Polymer Engineering & Science*, *25*(9), 535-540
15 . Ram, A., Zilber, O., & Kenig, S. (1985). Residual stresses and toughness of polycarbonate exposed to environmental conditions. *Polymer Engineering & Science*, *25*(9), 577-581
16 . Sherman, E. S., Ram, A., & Kenig, S. (1982). Tensile failure of weathered polycarbonate. *Polymer Engineering & Science*, *22*(8), 457-465.
17 . Tjandraatmadja, G. F., Burn, L. S., & Jollands, M. C. (2002). Evaluation of commercial polycarbonate optical properties after QUV-A radiation—the role of humidity in photodegradation. *Polymer degradation and stability*, *78*(3), 435-448

18 . Shamsundara, B. V., Mannikar, A. V., & Shridhar, T. N. (2011). Study on Polymer Degradation due to Weathering and its Effect on Vehicle Safety (No. 2011-26-0097). SAE Technical Paper
19 . Tocháček, J., & Vrátníčková, Z. (2014). Polymer life-time prediction: The role of temperature in UV accelerated ageing of polypropylene and its copolymers. *Polymer Testing*, *36*, 82-87
20 . Miller, D. C., Carloni, J. D., Johnson, D. K., Pankow, J. W., Gjersing, E. L., To, B., ... & Kurtz, S. R. (2013). An investigation of the changes in poly (methyl methacrylate) specimens after exposure to ultra-violet light, heat, and humidity. *Solar energy materials and solar cells*, *111*, 165-180
21 . Shioda, T. (2011, September). UV-accelerated test based on analysis of field-exposed PV modules. In *Reliability of Photovoltaic Cells, Modules, Components, and Systems IV* (Vol. 8112, p. 81120I). International Society for Optics and Photonics
22 . Poisson, C., Hervais, V., Lacrampe, M. F., & Krawczak, P. (2006). Optimization of PE/binder/PA extrusion blow-molded films. II. Adhesion properties improvement using binder/EVA blends. *Journal of applied polymer science*, *101*(1), 118-127
23 . Awaja, F., Gilbert, M., Kelly, G., Fox, B., & Pigram, P. J. (2009). Adhesion of polymers. *Progress in polymer science*, *34*(9), 948-968
24 . Hochrein, T., & Alig, I. (2011). Prozessmesstechnik in der Kunststoffaufbereitung (process measurement techniques for plastics compounding). *Vogel-Verlag, Wuerzburg*
25 . Botos, J., Murail, N., Heidemeyer, P., Kretschmer, K., Ulmer, B., Zentgraf, T., ... & Hochrein, T. (2014, May). Color measurement of plastics-From compounding via pelletizing, up to injection molding and extrusion. In *AIP Conference Proceedings* (Vol. 1593, No. 1, pp. 16-19). American Institute of Physics
26 . Botos, J., Murail, N., Heidemeyer, P., Kretschmer, K., Ulmer, B., Zentgraf, T., ... & Hochrein, T. (2014, May). Color measurement of plastics-From compounding via pelletizing, up to injection molding and extrusion. In *AIP Conference Proceedings* (Vol. 1593, No. 1, pp. 16-19). American Institute of Physics.
27 . A. Chrisment in Editions 3C Conseil, Paris, 1993
28 . Gok, A., Gordon, D. A., Wang, M., French, R. H., & Bruckman, L. S. (2019). Degradation Science and Pathways in PV Systems. In *Durability and Reliability of Polymers and Other Materials in Photovoltaic Modules* (pp. 47-93). William Andrew Publishing
29 . Andreassen, E., Larsen, Å., Nord-Varhaug, K., Skar, M., & Øysæd, H. (2002). Haze of polyethylene films—effects of material parameters and clarifying agents. *Polymer Engineering & Science*, *42*(5), 1082-1097.
30 . Sun, Z., Fan, H., Chen, Y., & Huang, J. (2018). Synthesis of self-matting waterborne polyurethane coatings with excellent transmittance. *Polymer International*, *67*(1), 78-84.][Vessot, K., Messier, P., Hyde, J. M., & Brown, C. A. (2015). Correlation between gloss reflectance and surface texture in photographic paper. *Scanning*, *37*(3), 204-217
31 . Yong, Q., Nian, F., Liao, B., Guo, Y., Huang, L., Wang, L., & Pang, H. (2017). Synthesis and surface analysis of self-matt coating based on waterborne polyurethane resin and study on the matt mechanism. *Polymer Bulletin*, *74*(4), 1061-1076.
32 . Elton, N. J., & Day, J. C. C. (2009). A reflectometer for the combined measurement of refractive index, microroughness, macroroughness and gloss of low-extinction surfaces. *Measurement Science and Technology*, *20*(2), 025309

APPENDIX

33 . Yong, Q., Chang, J., Liu, Q., Jiang, F., Wei, D., & Li, H. (2020). Matt Polyurethane Coating: Correlation of Surface Roughness on Measurement Length and Gloss. *Polymers*, *12*(2), 326
34 . Iannuzzi, G., Mattsson, B., & Rigdahl, M. (2013). Color changes due to thermal ageing and artificial weathering of pigmented and textured ABS. *Polymer Engineering & Science*, *53*(8), 1687-1695
35 . Yong, Q., Chang, J., Liu, Q., Jiang, F., Wei, D., & Li, H. (2020). Matt Polyurethane Coating: Correlation of Surface Roughness on Measurement Length and Gloss. *Polymers*, *12*(2), 326
36 . Juuti, M., Prykäri, T., Alarousu, E., Koivula, H., Myllys, M., Lähteelä, A., ... & Peiponen, K. E. (2007). Detection of local specular gloss and surface roughness from black prints. *Colloids and Surfaces A: Physicochemical and Engineering Aspects*, *299*(1-3), 101-108
37 . Yong, Q., & Liang, C. (2019). Synthesis of an Aqueous Self-Matting Acrylic Resin with Low Gloss and High Transparency via Controlling Surface Morphology. *Polymers*, *11*(2), 322
38 . Cawthorne, J. E., Joyce, M., & Fleming, D. (2003). Use of a chemically modified clay as a replacement for silica in matte coated ink-jet papers. *Journal of Coatings Technology*, *75*(937), 75-81
39 . Ou, J., Zhang, M., Liu, H., Zhang, L., & Pang, H. (2015). Matting films prepared from waterborne acrylic/micro-SiO2 blends. *Journal of Applied Polymer Science*, *132*(13)
40 . Bauer, F., Decker, U., Czihal, K., Mehnert, R., Riedel, C., Riemschneider, M., ... & Buchmeiser, M. R. (2009). UV curing and matting of acrylate nanocomposite coatings by 172 nm excimer irradiation. *Progress in Organic Coatings*, *64*(4), 474-481
41 . Lin, H., Wang, Y., Gan, Y., Hou, H., Yin, J., & Jiang, X. (2015). Simultaneous formation of a self-wrinkled surface and silver nanoparticles on a functional photocuring coating. *Langmuir*, *31*(43), 11800-11808
42 . Tjandraatmadja, G. F., Burn, L. S., & Jollands, M. C. (2002). Evaluation of commercial polycarbonate optical properties after QUV-A radiation—the role of humidity in photodegradation. *Polymer degradation and stability*, *78*(3), 435-448
43 . De Chiffre, L., Lonardo, P., Trumpold, H., Lucca, D. A., Goch, G., Brown, C. A., ... & Hansen, H. N. (2000). Quantitative characterisation of surface texture. *CIRP Annals*, *49*(2), 635-652
44 . Blateyron, F. (2013). The areal field parameters. In *Characterisation of areal surface texture* (pp. 15-43). Springer, Berlin, Heidelberg
45 . ISO, I. (2012). 25178-2: 2012—Geometrical Product Specifications (GPS)—Surface Texture: Areal—Part 2: Terms, Definitions and Surface Texture Parameters. *International Standards Organization: Geneva, Switzerland*
46 . Downey, T. (2016). *A computational analysis of the application of skewness and kurtosis to corrugated and abraded surfaces* (Doctoral dissertation, Memorial University of Newfoundland)
47 . Blateyron, F. (2013). The areal field parameters. In *Characterisation of areal surface texture* (pp. 15-43). Springer, Berlin, Heidelberg
48 . Nair, A., Sharma, P., Sharma, V., & Diwan, P. K. (2020). Effect of UV-irradiation on the optical properties of transparent PET polymeric foils. *Materials Today: Proceedings*, *21*, 2105-2111

49 . Gok, A., Ngendahimana, D. K., Fagerholm, C. L., French, R. H., Sun, J., & Bruckman, L. S. (2017). Predictive models of poly (ethylene-terephthalate) film degradation under multi-factor accelerated weathering exposures. *PloS one*, *12*(5), e0177614
50 . Standard, A. S. T. M. (2012). G173-03-Standard Tables for Reference Solar Spectral Irradiances: Direct Normal and Hemispherical on 37 Tilted Surface. *Ann. Book of ASTM Standards 2003*, *14*, 1-20.
51 . ASTM G154-16, Standard Practice for Operating Fluorescent Ultraviolet (UV) Lamp Apparatus for Exposure of Nonmetallic Materials. West Conshohocken, PA: ASTM International; 2016.
52 . Gok, A., Ngendahimana, D. K., Fagerholm, C. L., French, R. H., Sun, J., & Bruckman, L. S. (2017). Predictive models of poly (ethylene-terephthalate) film degradation under multi-factor accelerated weathering exposures. *PloS one*, *12*(5), e0177614
53 . J.F. Rabek, Polymer Photodegradation - Mechanisms and Experimental Methods, Chapman & Hall, London, UK (1995).
54 . J.G. Borkia and S. Schlick, Polymers, 43, 3239 (2002).
55 . R.M. Santos, G.L. Botelho, and A.V. Machado, J. Appl. Polym. Sci., 116, 2005 (2010)
56 . J.F. Rabek, ‘‘Photochemical Aspects of Degradation of Polymers,’’ Polymer Photodegradation - Mechanisms and Experimental Methods, Chapman & Hall, London, UK (1995)
57 . B.E. Tiganis, L.S. Burn, P. Davis, and A.J. Hill, Polym. Degrad. Stab., 76, 425 (2002).
58 . J. Shimada and K. Kabuki, J. Appl. Polym. Sci., 12, 655 (1968).
59 . J. Shimada and K. Kabuki, J. Appl. Polym. Sci., 12, 671 (1968).
60 . J.F. Rabek, ‘‘Photodegradation and Photo-oxidative Degra- dation of Homochain Polymers,’’ Polymer Photodegradation - Mechanisms and Experimental Methods, Chapman & Hall, London, UK (1995).
61 . Iannuzzi, G., Mattsson, B., & Rigdahl, M. (2013). Color changes due to thermal ageing and artificial weathering of pigmented and textured ABS. Polymer Engineering & Science, 53(8), 1687-1695
62 . Shimada, J., & Kabuki, K. (1968). The mechanism of oxidative degradation of ABS resin. Part I. The mechanism of thermooxidative degradation. *Journal of Applied Polymer Science*, *12*(4), 655-669
63 . Boldizar, A., & Möller, K. (2003). Degradation of ABS during repeated processing and accelerated ageing. *Polymer degradation and stability*, *81*(2), 359-366.
64 . Ashby, M. F., & Cebon, D. (1993). Materials selection in mechanical design. *Le Journal de Physique IV*, *3*(C7), C7-1
65 . Altuglas International Plexiglas UF-3 UF-4 and UF-5 sheets, 2006-11-17 at the Wayback Machine. Plexiglas.com. Retrieved 2012-05-09.
66 . *Andrei, D., Ana-Maria, A., Claudiu, B., Oana, C., & Liviu, U. (2018). OBTAINING COMPOSITE MATERIALS OF THE POLYMER-ALUMINIUM TYPE BY GLUING USING BICOMPONENT ADHESIVES. International Multidisciplinary Scientific GeoConference: SGEM, 18(6.1), 355-362*
67 . Wypych, G. (2016). *Handbook of polymers*. Elsevier
68 . Data from Torikai, A; Hasegawa, H, Polym. Deg. Stab., 61, 2, 361-4, 1998.
69 . Wypych, G. (2016). *Handbook of polymers*. Elsevier
70 . Miller, D. C., Gedvilas, L. M., To, B., Kennedy, C. E., & Kurtz, S. R. (2010, August). Durability of poly (methyl methacrylate) lenses used in concentrating photovoltaic modules.

APPENDIX

In *Reliability of Photovoltaic Cells, Modules, Components, and Systems III* (Vol. 7773, p. 777303). International Society for Optics and Photonics
71 . Miller, D. C., Carloni, J. D., Johnson, D. K., Pankow, J. W., Gjersing, E. L., To, B., ... & Kurtz, S. R. (2013). An investigation of the changes in poly (methyl methacrylate) specimens after exposure to ultra-violet light, heat, and humidity. *Solar energy materials and solar cells*, *111*, 165-180.
72 . Seubert, C., Nietering, K., Nichols, M., Wykoff, R., & Bollin, S. (2012). An overview of the scratch resistance of automotive coatings: exterior clearcoats and polycarbonate hardcoats. *Coatings*, *2*(4), 221-234
73 . Pickett, J. E., Gibson, D. A., & Gardner, M. M. (2008). Effects of irradiation conditions on the weathering of engineering thermoplastics. *Polymer Degradation and Stability*, *93*(8), 1597-1606.
74 . Brennan P, Fedor C. Sunlight, UV, and accelerated weathering. Surface Coatings Australia 1988:7–11
75 . Tjandraatmadja, G. F., Burn, L. S., & Jollands, M. C. (2002). Evaluation of commercial polycarbonate optical properties after QUV-A radiation—the role of humidity in photodegradation. *Polymer degradation and stability*, *78*(3), 435-448
76 . American Society for Testing and Materials. Test method for specular gloss of plastic films and solid plastics, vol. 8.02. ASTM D2457–97. Philadelphia: ASTM; 1997
77 . Guerrero, H., Rosa, G., Morales, M. P., Del Monte, F., Moreno, E. M., Levy, D., ... & Serna, C. J. (1997). Faraday rotation in magnetic γ-Fe 2 O 3/SiO 2 nanocomposites. *Applied physics letters*, *71*(18), 2698-2700
78 . Vu-Khanh, T., Sanschagrin, B., & Fisa, B. (1985). Fracture of mica-reinforced polypropylene: Mica concentration effect. *Polymer composites*, *6*(4), 249-260.
79 . Meeten, G. H. (1986). Optical properties of polymers. *Elsevier Applied Science Publishers Ltd, Crown House, Linton Road, Barking, Essex IG 11 8 JU, UK, 1986*
80 . Zhou, R. J., & Burkhart, T. (2010). Optical properties of particle-filled polycarbonate, polystyrene, and poly (methyl methacrylate) composites. *Journal of applied polymer science*, *115*(3), 1866-1872.]
81 . Seubert, C., Nietering, K., Nichols, M., Wykoff, R., & Bollin, S. (2012). An overview of the scratch resistance of automotive coatings: exterior clearcoats and polycarbonate hardcoats. *Coatings*, *2*(4), 221-234